REPORT DOCUMENTATION PAGE

Form Approved OMB No. 0704-0188

1. AGENCY USE ONLY (Leave blank)	2. REPORT DATE	3. REPORT TYPE AND DATES COVERED
	1995	Final Report

4. TITLE AND SUBTITLE

Near-Regional Ground Motions

5. FUNDING NUMBERS

F6170894W0749

6. AUTHOR(S)

Dr. I Kitov

7. PERFORMING ORGANIZATION NAME(S) AND ADDRESS(ES)

Russian Academy of Sciences
Lenininsky Prospekt, 18
Kopus 6
Moscow 11797
Russia

8. PERFORMING ORGANIZATION REPORT NUMBER

N/A

9. SPONSORING/MONITORING AGENCY NAME(S) AND ADDRESS(ES)

EOARD
PSC 802 BOX 14
FPO 09499-0200

10. SPONSORING/MONITORING AGENCY REPORT NUMBER

SPC 94-4064

11. SUPPLEMENTARY NOTES

12a. DISTRIBUTION/AVAILABILITY STATEMENT

Approved for public release; distribution is unlimited.

12b. DISTRIBUTION CODE

A

13. ABSTRACT (Maximum 200 words)

Record seismic and acoustic waves by blasts of different energy released at different heights. The data processing includes amplitute, period and spectral estimations of different seismic and acoustic phases, their interpretation and definition of the dependence of the observed characteristics on explosion yield, height of burst and the subsurface geology of the test area.

14. SUBJECT TERMS

Nil

15. NUMBER OF PAGES

48

16. PRICE CODE

N/A

17. SECURITY CLASSIFICATION OF REPORT	18. SECURITY CLASSIFICATION OF THIS PAGE	19. SECURITY CLASSIFICATION OF ABSTRACT	20. LIMITATION OF ABSTRACT
UNCLASSIFIED	UNCLASSIFIED	UNCLASSIFIED	UL

INSTITUTE FOR DYNAMICS OF THE GEOSPHERES

ACADEMY OF SCIENCES, RUSSIAN REDERATION

Leninsky Prospect, 38

Korpus 6

Moscow, Russia 117979

Sponsored by EOARD (AFOSR)

Contract SPC-94-4064

FINAL REPORT

Near-Regional Ground Motions

Principal Investigator: Ivan O. Kitov

Moscow, 1995

Abstract

Scientists from the Institute for Dynamics of the Geospheres carried out a series of 8 explosive tests in December 1985 at a Soviet bombing range near Kustanai, Kazakhstan. The objective of the experiments was to record seismic and acoustic waves by blasts of different energy release at different heights. The charges were conventional bombs with total weights of 3000, 1500 and 500 kg. The chemical explosives constituted about 50% of the weights of the bombs. The series consisted of five 1500 height of burst tests (2 at 8 km, 2 at 6 km, 1 at 4 km) and three near-surface explosions with weights of 500, 1500 and 3000 kg. The 500 kg and 3000 kg explosions detonated on impact, while the 1500 kg explosion had a 1 sec delay which resulted in a penetration to a depth of about 15 m in the marshy soil. There were three observation points at ranges 6, 9.5 and 21 km. All three ground motion components (R, T, Z) were measured at all the three ranges. In addition, acoustic sensors (microphones) were installed at each point. At 6 km the sensor was at the top of a tower of about 7 m height. AT 9.5 km there were two sensors at heights of 1 and 13 m and at 21 km there were two different sensors at a height of about 1 m. Excellent seismic and acoustic data were recorded from these tests and they show evidence of a variety of potentially diagnostic phenomena.

The seismic and acoustic data were measured by conventional oscilloscopes onto the photographic paper. At first, the data were digitized and converted into standard format to access the data processing options. All the digitized waveforms with proper description were assemled into a uniform database, which is available now to seismic verification community by prompt from the IDG. There are more than 50 3-C seismic and acoustic recordings.

The data processing included amplitude, period and spectral estimations of different seismic and acoustic phases, their interpretation and definition of the dependence of the observed characteristics on explosion yield, height of burst and the subsurface geology of the test area. The atmospheric and near-surface explosions generate different seismic phases. The most prominent are the air-coupled surface wave generated locally, and the Airy phase which propagates with alsmost constant period and relatively low attenuation. The atmospheric explosions generate the air-coupled wave relatively more efficient than the near-surface with a ratio of the amplitudes of the waves being more than an order of magnitude higher from the atmospheric explosions. This feature shows evidence of difference between atmospheric and near-surface explosions.

Second prominent feature of the near-surface explosions is a large-amplitude acoustic wavetrain arriving after the first impulsive arrival. This wavetrain is generated near the sources by constructive interference induced by the surface wave harmonics with phase velocity equal to the sound velocity in the air. There is no such an arrival from the atmospheric explosions.

There is also another signature of the observed acoustic waves important for discrimination. The atmospheric explosions of the bombs generate a relatively intensive high-frequency precursor associated with supersonic ejection of shell splinters and related low amplitude impulses arrival. The

contained explosion did not show such a signature due to no shell splinters ejected.

The observed seismic waves from the atmospheric explosions show a possibility of using them to estimate height of burst. There are some procedures of the HOB estimation proposed in the study based on arrival times of different phases, dispersion of the air-coupled wave, and time duration of the signals.

A phase velocity dispersion curve was estimated from the observed periods in the air-coupled wave and the apparent velocities of the acoustic wave along the free surface. The curve is consisted with a theoretical curve, calculated from the known velocity distribution in the local geological structure.

Spectral processing showed that the Airy phase has a period of about 1 sec consistent with the thickness of the sedimentary layer and seismic waves' velocities in the geological structure. The air-coupled wave is characterized by a variation of the periods due to changes of the apparent velocity of the acoustic front along the free surface.

Table of Contents

INTRODUCTION

Explosion sources above the free surface generate different types of waves in the solid Earth and atmosphere, and some interesting processes of energy conversion can occure at the interface between the ground and the air. For example, an acoustic wave moving along the surface can generate very efficiently coupled seismic waves then there is a surface wave harmonic with phase velocity equal to apparent acoustic front velocity. Similarly, seismic surface wave can generate an inhomogeneous acoustic wave train above the free surface if its phase velocity equal to sound speed in the air. These effects depend on the local velocity structure and are of significant interest since the data can be used in a variety of scientific and practical applications.

Air coupled surface waves from airblasts and surface explosions, as well as the exitation of acoustic waves by low velocity Rayleigh waves, have been studied during the last forty years. Theoretical and experimental aspects of this problem have been thoroughly discussed in Press and Oliver (1955) and by Ewing et al. (1957). Strong motion surface waves generated in the epicentral zone of near surface explosion and a multiply surface blast has been modeled by Murphy (1981, 1988). The possibility of locating acoustic wave sources, such as aircraft crashes and meteorite impacts has been demonstarated by Johnston (1987). Some soil dynamics problems associated with propagating air pressure waves were discussed by Werkle and Waas (1987).

This study is devoted to the discussion of experimental results obtained during a series of bomb explosions which were detonated above and below the free surface at a selected site.

DESCRIPTION OF THE EXPERIMENT

Seismic and acoustic data were measured from a series of eight explosive tests which were carried out in December, 1985, at a site located at the north-west edge of the Kazakh platform near the Turan depression. The total weights of the bombs ranged from 500 to 3000 kg with the weight of explosive estimated to be of 0.5-0.6 of the total weight. Naturally, a bomb explosion is different from a standard chemical blast due to the effect of the metallic shell, and so the the estimation of the yield from the charge weight may be confusing. Moreover, shell-splinter ejection produces additional sources of acoustic wave generation, as will be discussed below. Table 1 summarizes the conditions of all the experiments (altitude or depth and weight of the bomb). Five explosions were detonated above the ground in the altitude range from 4000 to 8000 m, two explosions were at the surface and one explosion was dropped over a swamp-like environment and had an estimated depth of penetration of about 15 m at the time of detonation.

All the explosions were detonated in winter time during two days in which the near surface air temperature was -10 °C. The thickness of the snow layer beneath the blasts was in the range from 10 to 100 cm along the profile of portable seismic stations and the frozen soil layer had the thickness of 30-40 cm. The sound velocity for this temperature was calculated from the relationship $c_a = 20\sqrt{T}$, where T is in °K, and was of approximately 320 m/s. Due to the absence of data on shot times and precise locations in these experiments we could not estimate sound speed from the recorded data.

A profile of portable sensors was installed to record seismic and acoustic waves generated by the blasts over the epicentaral distance range from about 6 to 21 km. Three-component seismic sensors were deployed at distances 6, 9.5 and 21 km with the two horizontal components oriented radial and transverse with respect to the source location. Acoustic sensors were installed at heights from 1 to 7 m at the 6 and 21 km stations and two sensors at the heights of 1 and 13 m were

employed at the 9.5 km station. The profile configuration scheme is summarized in Figure 1.

Seismic data were recorded using standard short period sensors SM-3 and S5-S, with recording on photographic paper using the OMS-3M oscilloscope. The nominal seismic channel response is presented in Figure 2. Specially designed microphones with the responces presented in Figure 3 were used to record the acoustic wave. The equipment sensitivity was adjusted in order to record the seismic and acoustic waves over the wide dynamic range associated with different types of blasts.

The measured seismic and acoustic waveforms are summarized in Appendix A, where all the records are presented with regarding descriptive information.

Table 1. Source positions and bomb weights

N	m,kg	h,m
1	500	0
2	1500	-15
3	1500	4000
4	1500	6000
5	1500	6000
6	3000	0
7	1500	8000
8	1500	8000

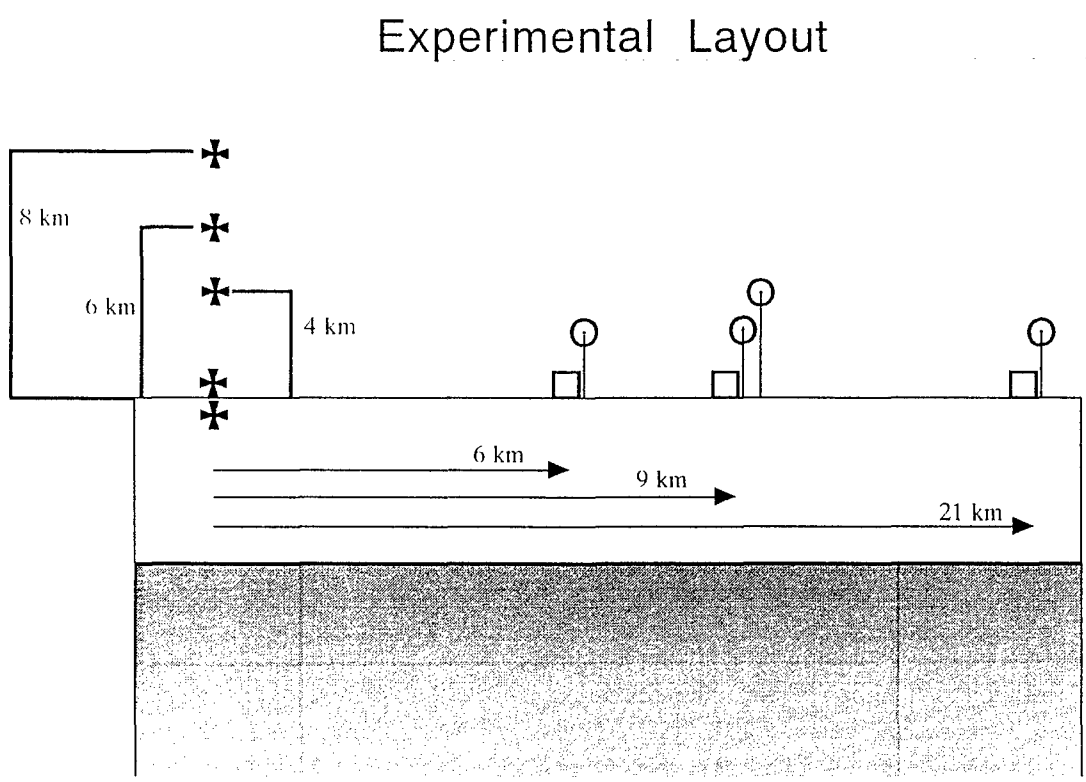

Figure 1. Experimental layout: crosses - blasts, squares - seismic station, circles - acoustic sensors

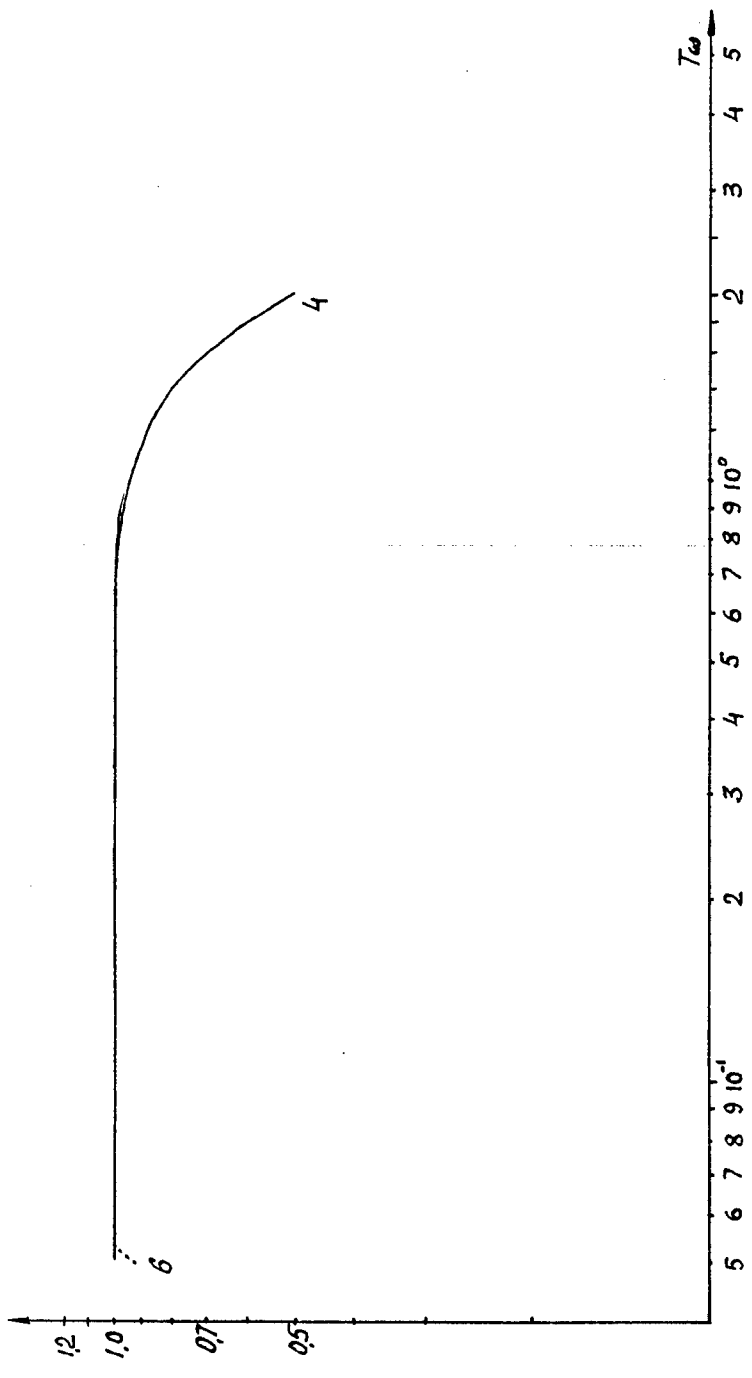

Figure 2. Standard normalized seismic channel responce (curve 4).

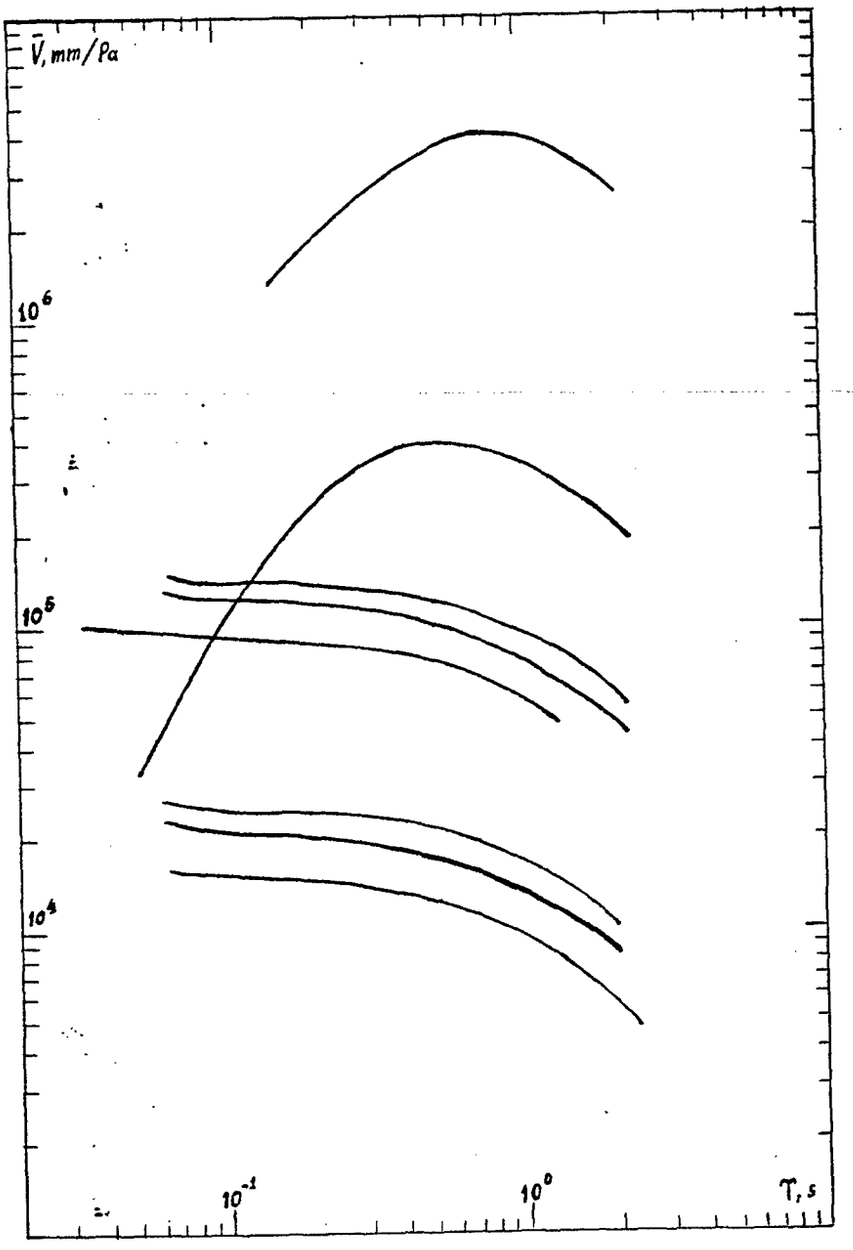

Figure 3. Standard acoustic channel responces, V - amplification factor in mm/Pa, T - period in seconds.

LOCAL GEOLOGY

We have adopted a three layer velocity model to interpret the observed wave-field. This model is related to geological structure obtained from different literature sources. The top layer of unconsolidated clay and sand has a thickness of 40-55 m with shear wave velocity β_1=0.30 km/s and compressional wave velocity α_1=0.8 km/s. The second layer of sediments has a thickness of 350-400 m with of β_2=0.95 km/s and α_2=2.05 km/s. The third layer represents intrusive rocks with β_3=2.5 km/s and α_3=4.6 km/s and is assumed to have infinite extent. These estimates are taken from Berzon and Pasechnik (1976). The assumed infinite thickness of the third layer implies that the surface waves we measured are concentrated in the two upper layers and the thickness of the third layer does not influence the observed propagation effects.

THEORETICAL BACKGROUND

Two principal effects of Rayleigh surface wave exitation and propagation should be considered for the case of acoustic wave interaction with the layered structure described above. The first is constructive interference of Rayleigh surface waves with phase velocity equal to apparent acoustic wave velocity along the free surface. This effect is very important in the present the case due to the existance of a low velocity surface layer with shear velocity approximately equal to the sonic velocity, as well as the fact that the altitudes of the blasts provide apparent acoustic front velocities from infinity near the epicenter to sonic velocity at large distances.

Ewing et al. (1957) derived a period equation for the case of non-zero air density in the interaction of acoustic and seismic waves. This period equation contains terms which include the expression $\rho_o/\rho_1 n_o$, where ρ_o is the air density, ρ_1 is the ground density and $n_o=(1-c^2/c_a^2)^{1/2}$ where c is the phase velocity of surface wave, c_a is the sonic wave speed. The corresponding group velocity dispersion curve is represented by three branches. The first branch is the usual Rayleigh wave with normal dispersion which propagetes with a velocity corresponding to the third layer. The second branch corresponds to surface wave propagating in the upper layers. These two branches merge at some frequency of minimum group velocity associated with an Airy phase propagating with almost constant period. The third branch corresponds to the coupling of the Rayleigh wave to an atmospheric compressional wave. The frequency of this wavetrain is almost constant and its arrival is associated with the acoustic wave. The phase velocity in this surface wave is close to the acoustic front apparent velocity. If $c>c_a$, n_o becomes complex and this represents a radiation of energy from ground to air.

The second effect is associated with the relative efficiency of propagation of the different harmonics of the Rayleigh wave. Due to the strong differentiation of geological structure and associated shear velocity changes of a factor of 3 at the

interfaces, the group velocity curve has two deep minima. Thus, Rayleigh wave motion has to be dominated by frequency components associated with group velocity minima (Levshin, 1973; Murphy and Shah, 1988) or Airy phases. The Airy phase geometrical spreading factor is lower than that of other harmonics ($r^{-5/6}$ and r^{-1}, respectively) due to smaller duration of the wavetrain (Levshin, 1973). Therefore, one can expect almost constant frequency surface wave at larger distances, where all harmonics other than those related to the Airy phase have attenuated. The Airy phase corresponding to the upper layer attenuates with distance more rapidly due to lower group velocity and lower quality factor, Q. Thus, only one Airy phase can be detected at large range.

ACOUSTIC WAVES FROM AIR-BLASTS

Acoustic wave generation by air-blasts has been studied thoroughly both experimentally and theoretically. The only unusual features in this case are due to the metallic bomb casing which reduces the efficiency of the blast as a result of work done in fragmenting of the casing and also provides additional sources of acoustic wave during shell-splinter ejection. Shell-splinters initially have velocities in the 1.0 to 2.4 km/s range and gradually decelerate due to air friction. Since the initial speed is greater than the sound velocity, a shock wave arises behind the tip. The shock wave detaches as the shell-splinter slows down and propagates as a pulse to the receiver. This effect is clear from the records presented in Figure 4. The main features of this "precursor" are the amplitude growth before the main shock arrival and a time duration approximately one second before the to 0.5 seconds after the principal wave arrival. The duration of this signal is determined by the maximum initial shell-splinter velocity and the directivity of debris ejection and does not depend on the receiver position. The arrivals after the principal shock are associated with the shell-splinters which have trajectories away from the direction to the reciever. The hypotesis of such a mechanism for the precursor generation is supported by the absence of an observed precursor on the recordings of the tamped explosion.

The measured values of relative pressure in the acoustic waves from the air-blasts are presented in Table 2. We have used the experimentally derived relationship (Gubkin, 1978):

$$\Delta P(r) = 13.5 \frac{q^{1/3}}{r[\ln(r/27q^{1/3}]^{1/2}} \qquad (1)$$

in order to estimate pressure (in Pa) in the acoustic wave at distance r (in km) from a blast of total energy q, with q measured in tons of TNT. The calculated values are also

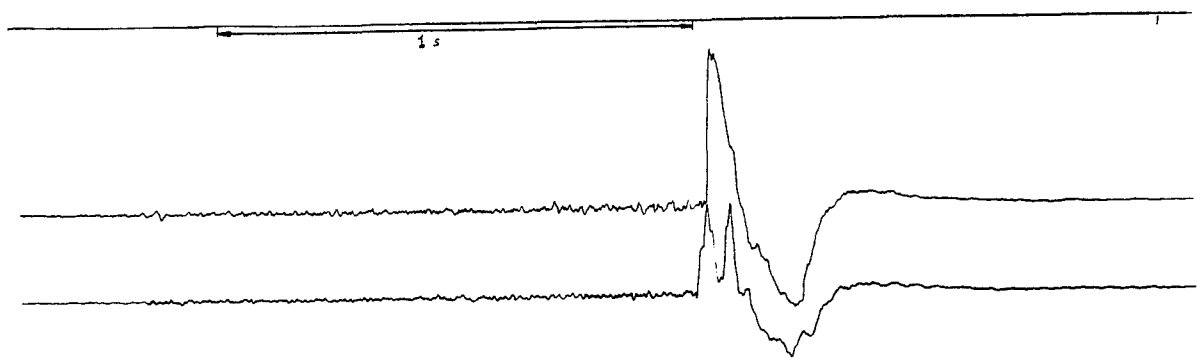

Figure 4. Acoustic signals recorded at the heights of 1 and 13 m. Double peaked arrival relates to transient and reflected wave. High frequency oscillations before the main shock are generated by iron shell fragments supersonic flight.

presented in Table 2 and coinside relatively well with observed, if uncertainties due to influence of height of burst and sound speed distribution are taken into consideration.

At the epicentral distance of 9.5 km there were two acoustic sensors at heights of 1 and 13 m. The records at this point are shown in Figure 4 where it can been seen that the sum of the pressures in the incident and reflected waves at the height of 1 m is approximately equal to twice the pressure in the incident wave at the height of 13 m, as expected.

The spectral characteristics of the acoustic waves can be inferred from the positive and negative phase durations presented in Table 2. It can be seen that the positive phase of the acoustic wave has a duration of 0.06 s at the distance of 9.5 km and 0.26 s at 21 km. The negative phase duration is longer at about 0.5 s, which is close to the observed period of the air-coupled Rayleigh wave. Thus, the spectral composition of the acoustic and surface waves are similar which makes the process of energy transfer more effective.

Table 2. Measured and calculated parameters of acoustic wave (yield for calculations is 1 ton TNT)

h,km	R,km	ΔP, Pa measured	ΔP, Pa calcul.	τ_+, sec	τ_-, sec
4	10	170	112	0.06	0.5
4	21	50	52	0.26	-
6	10	170	100	0.06	0.5
6	21	52	50	0.25	-
8	10	140	82	0.06	0.5
8	21	12	46	0.29	-

SEISMIC OBSERVATIONS

Atmospheric, surface and tamped explosions have different efficiency of seismic wave exitation. The most efficient seismic wave generation is assocoated with the 1 ton buried explosion, although the surface explosions are also relatively efficent seismic sources. The seismic waves observed from the atmospheric blasts, however, are dominant by the air-coupled surface wave components of the motion.

Body waves

Only the most distant station at 21 km recorded body waves from the tamped and surface explosions due to the fact that the recordings at the closer stations were not initiated soon enouth due to technical problems. Figure 5 shows the initial part of the seismogram recorded at 21 km station from the explosion of the 3 tons surface exploion and it can be seen that it shows a distinct P-wave arrival. A weaker signal can be seen arriving about 1 sec before the principal P-wave arrival on this figure and it seems likely that this is associated with the bomb impact on the surface, since the detonation time was delayed by about 1 sec with respect to the impact time in this case to permit penetration beneath the surface. Although it is not possible to estimate a precise velocity for the initial P arrival in the absence of an accurate origin time, its relative time of arrival with respect to the acoustic wave suggests it is a refracted arrival time from the underlying rock layer characterized by α_3=4.6 km/sec.

Surface waves

The most prominent phases of the observed surface waves are associated with propagation in the upper low velocity layers. The tamped and surface explosions produced broadband surface waves harmonics with periods raging from 2 to 0.3 s and group velocities ranging from 900 m/s to 30 m/s. The atmospheric

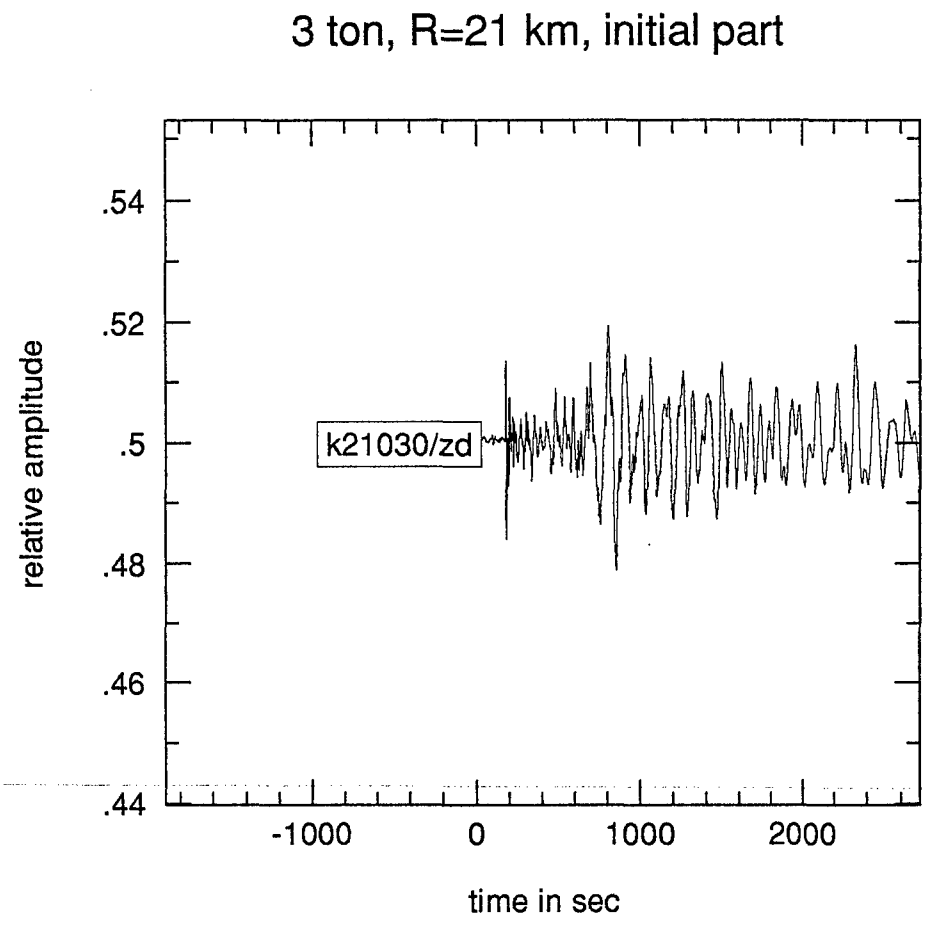

Figure 5. Initial part of vertical and radial channels of displacement. One second before blast generated P-wave arrives low amplitude P-wave from the bomb impact. Designed time delay was of 1 sec.

blasts chiefly produce air-coupled surface waves with phase velocities greater than 320 m/s. The apparent acoustic wave velocity along the surface depends on the height of the source (h) and epicentral distance (r) by relation

$$v_a = c_a \frac{(h^2+r^2)^{1/2}}{r} \qquad (2)$$

It follows that the gradient of the apparent velocity with respect to range is given by

$$\frac{dv_a}{dr} = - \frac{h^2}{r^2(h^2+r^2)^{1/2}} \qquad (3)$$

Two important consequences follow from Equations (2) and (3). First, the distance at which the same apparent acoustic velocity along the surface will be observed from blasts at different is proportional to height. Hence, since the upper limit of the phase velocity of the surface waves is equal to β_3, constructive interference can occur only beyond some distance $r_o(h)$ from the epicenter. Second, the gradient of the acoustic front velocity for a given value of phase velocity decreases with increasing height. It follows that since the velocity gradient along the surface determines the duration of constructive interference with the surface components having velocities close to the apparent acoustic wave velocity, the relative amplitude of the air-coupled surface wave component is proportional to source height if the acoustic wave amplitude is constant. Since the low amplitude acoustic wave amplitude decreases more rapidly than r^{-1} there should be some maximum in the air-coupled surface wave amplitude/height relation. Moreover, the exponential distribution of air density in the atmosphere will tend to shift this maximum to lower height.

It follows from the above discussion that one can identify four different zones of surface wave exitation by the acoustic waves produced by atmospheric explosions.

(1) The first zone corresponds to apparent acoustic wave velocity larger than the maximum surface wave phase velocity possible in the region under consideration. The radius of this zone increases proportionally to height and in our case r_o=0.11h. Constructive interference in this zone is impossible and surface waves exitation is not very efficient.

(2) The second zone is distinguished by the relation between the apparent acoustic wave velocity and the group velocity of the exited surface waves. If the latter is lower, the acoustic front arrives before all the surface wave harmonics. This is the case for all the blasts recorded at the distance of 6 km and for the 8 km height blast recorded at the distance of 10 km. Figure 6 displays these records and no surface wave are seen before the acoustic front arrival in this cases.

(3) The third zone corresponds to the region where the higher group velocity surface waves arrive before the acoustic front. This pattern is illustrated in Figure 7 for the blasts at 4 and 6 km altitude recorded at the 10 km station. It can be seen that the acoustic front arrives about 1 to 2.5 sec after the surface wave for the blasts at heights of 6 and 4 km, respectively. Thus, the third zone is characterized by transient processes of exitation and dispersion of surface waves.

(4) The fourth and last zone correspods to the region where the two main surface wave phases are well separated. This is illustrated in Figure 8 using the recordings from the 21 km station. The two principal groups here are the Airy phase with group velocity of 400-450 m/s and an air-coupled wave with phase velocity equal to the apparent acoustic wave speed. The Airy phase attenuation is relatively low and, consequently, it can be recorded at larger distances, while the other harmonics attenuate more rapidly and become relatively smaller with increasing distance. The air-coupled surface wave attenuates very rapidly and progresses only locally.

Two important features of the surface waves in the second

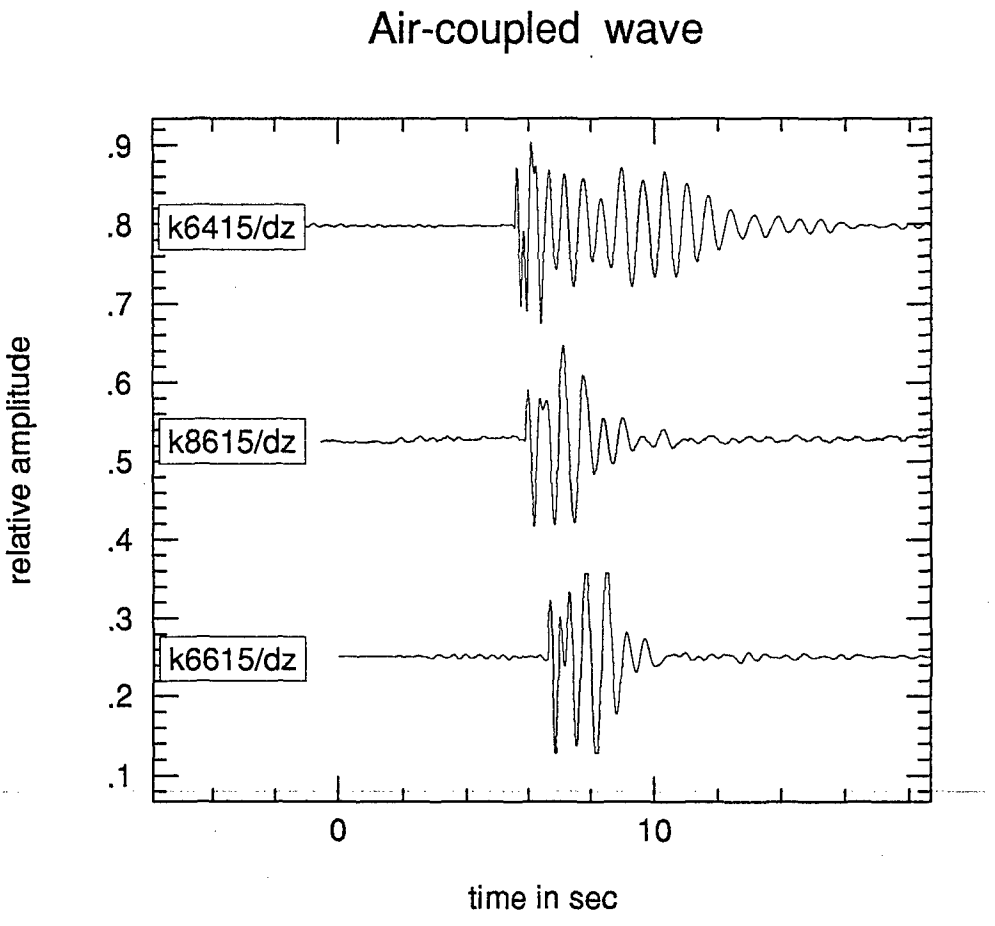

Figure 6. Air-coupled surface waves recorded at the distance of 6 km from the epicenter of the blasts at the heights of 4, 6 and 8 km. Tags contain information about experiment: k - experiment identificator, first one or two digits are the distance (6 and 10 km), next digit is the height (4, 6 or 8 km), next two digits are the bomb weight (05, 15 and 30), /dz is vertical component of displacement.

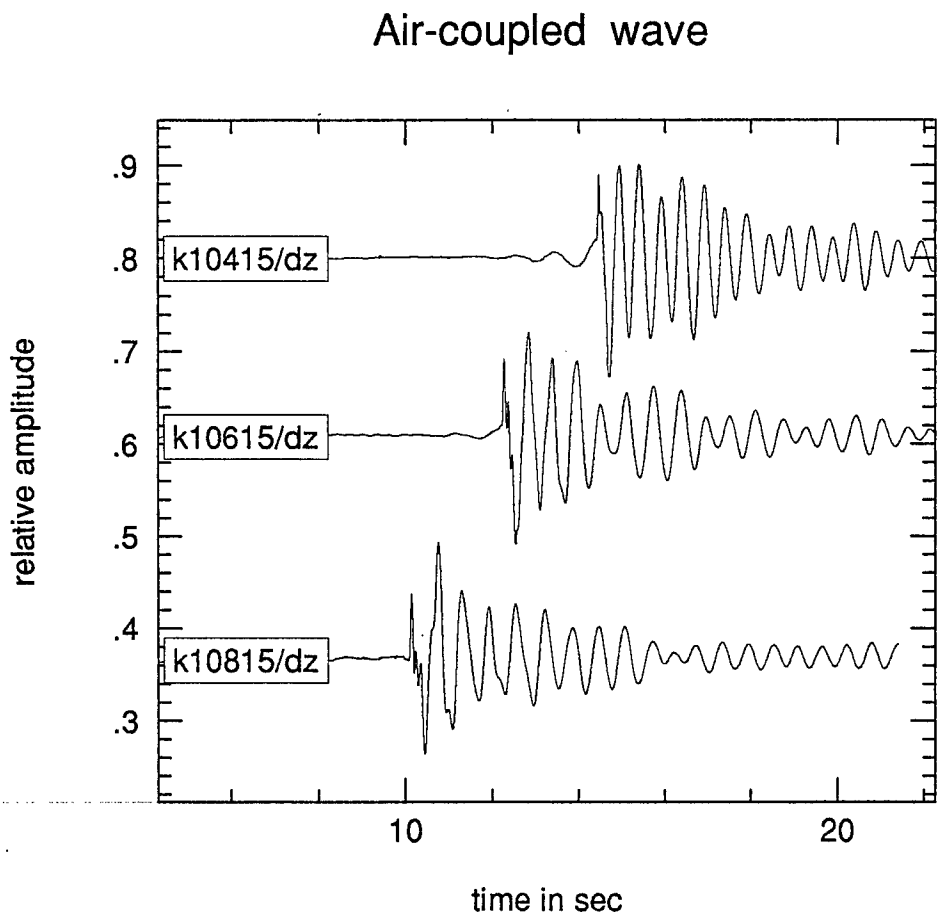

Figure 7. Air coupled surface waves recorded at the distance of 10 km from the epicenter of the blasts at the heights of 4 and 6 km. Tags are described in Fig. 6

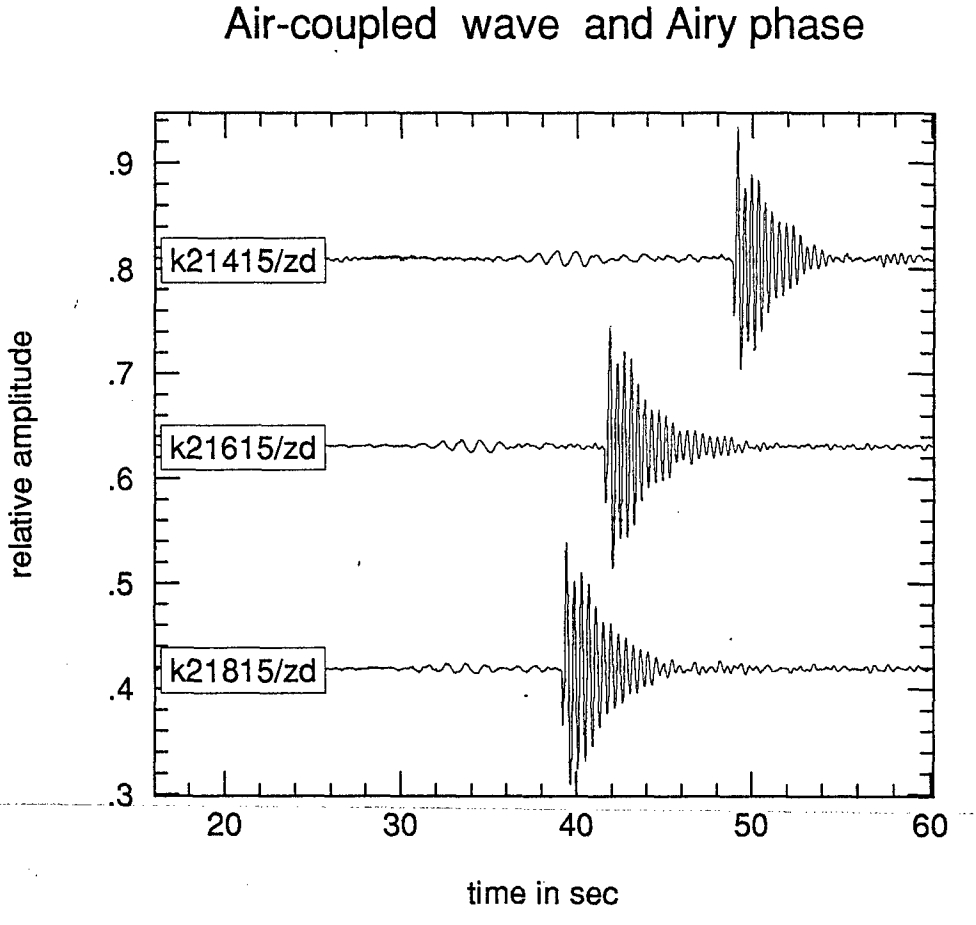

Figure 8. Air-coupled surface wave and Airy phase recorded at the distance of 21 km from all atmospheric blasts. Time interval between Airy phase and acoustic wave arrivals decreases with increasing height.

zone are signal duration and dispersion. The time duration depends on the distance from r_o to the receiver and the group velocity of the exited surface waves. For the blast at 4 km height, r_o is of about 0.5 km and for a group velocity of 500 m/s, the expected signal duration at the 6 km station is of the order of 11 sec, which is close to the measured value of 10.5 sec (cf. Figure 6). Similarly, a blast at 8 km height would be expected to produce a signal at 6 km distance with a duration of about 10 sec, assuming the minimum group velocity of 500 m/s. However, the observed signal duration for this case in Figure 6 is only about 5 sec, suggesting a higher effective group velocity for this component of the motion. The apparent dispersion in this zone is determined by the acoustic wave velocity gradient along the surface. Thus, low frequency harmonics with higher phase and group velocities are exited closer to the epicenter and lag behind the harmonics of higher frequency which are exited closer to the receiver. Hence, one can observe inverse dispersion or even more complicated pattern.

The fourth zone has the simpliest seismic wavefield. Here, the Airy phase has an almost constant period of about 1.0 sec and a time duration of 5-10 sec for the atmospheric explosions. The observed relative arrival times of the Airy phases are consistent with their group velocity of about 450 m/s and an initiation radius given by Equation (2). The observed peak displacement amplitudes for the vertical and radial components at 21 km station are presented in Table 3. It can be seen from this table that, for the atmospheric blasts, there is an amplitude maximum at height of 6 km, consistent with the above discussion of the effect of source height on surface wave amplitude. A similar maximum is also observed at the closest station and has the same nature, since the Airy phase is generated close to the epicenter.

The measured values of vertical and radial displacement for the air-coupled Rayleigh waves are presented in Table 4. This wave has the highest amplitude at all the stations for the atmospheric blasts. The duration of this air-coupled wave depends on the incident amplitude and the anelastic attenuation characteristics of the midium.

Table 3. Airy phase displacement amplitudes

q	h,km	Az,mm	Ax, mm
500	0	$5.8\ 10^{-4}$	$7.1\ 10^{-4}$
1500	0	$7.8\ 10^{-3}$	$7.7\ 10^{-3}$
3000	0	$7.1\ 10^{-3}$	$9.8\ 10^{-3}$
1500	4	$1.7\ 10^{-4}$	$1.3\ 10^{-4}$
1500	6	$2.3\ 10^{-4}$	$1.5\ 10^{-4}$
1500	8	$2.0\ 10^{-4}$	$1.4\ 10^{-4}$

Table 4. Peak displacement amplitudes in air-coupled surface waves

h, km	R, km	Az, $x10^{-3}$mm	Ax, $x10^{-3}$mm
4	6	13.7	13.4
6	6	16.0	13.0
8	6	13.0	10.0
4	10	11.5	8.0
6	10	11.0	10.2

8	10	12.1	8.6
4	21	1.78	0.52
6	21	1.9	0.82
8	21	2.62	0.85

Relative Efficiency of Atmospheric, Surface and Tamped Blasts

Since the Airy phase was measured for all the types of blasts carried out in the experiment, one can compare relative exitation efficiency for this phase. Also, these data can be used to estimate the distance at which the Airy phase should be detectable from a 1 ton explosion. From Table 3, the Airy phase amplitude expected from a 1500 kg surface blast can be estimated by interpolating between the observed amplitudes for the 500 and 3000 kg surface blasts. Assuming first power yield scaling, the expected amplitude at 21 km is of about $3x10^{-6}$ m. Now the average observed Airy phase displacement at this range from the three atmospheric blasts is about $2x10^{-7}$m, which indicates that the relative Airy phase exitation efficiency for the surface blasts is about 15 times that of the atmospheric blasts. By comparison, it can be seen from Table 3 that the Airy phase exitation efficiency for the buried blast is about 40 times that of the atmospheric blasts. Since this explosion was not fully contained, this ratio may be even higher for well tamped explosions.

Using the measured Airy phase displacement amplitude at 21 km together with the nominal Airy phase geometrical spreading factor $r^{-5/6}$ and assuming an anelastic quality factor of 100 for the second layer where the Airy phase predominantly propagetes, it is possible to estimate the Airy phase amplitude as a function of distance for a tamped 1 ton blast at this site. Then, defining detectability as a signal-to-noise ratio of 2 at 1 Hz, the estimated maximum distance of detection for such an explosion is about 75 km for a noise level of $5x10^{-8}$ m and about

110 km for a noise level of $5x10^{-9}$ m. The Airy phase form atmospheric explosions can't be detected at distances larger than 50-60 km, but Johnston (1987) has shown that air-coupled surface wave can be detected at larger distances due to the low attenuation of the acoustic wave amplitude.

Phase Velocity Dispersion Curve

An approximate phase velocity dispersion curve for this site can be easily determined using the measured air-coupled surface wave data in conjunction with the known characteristics of the acoustic wave field. Thus, the dominant apparent periods of the air-coupled surface wave data observed at the three stations from the atmospheric blasts at heights of 4, 6 and 8 km can be measured and associated with phase velocities corresponding to the apparent acoustic wave velocities given by Equation (2). The result for the present case are shown in Figure 9 where it can been seen that the measured periods of the recorded surface waves vary over the range from 0.39 to 0.66 sec, with associated inferred phase velocities ranging from a minimum of 323 m/sec to a maximum of of 540 m/sec.

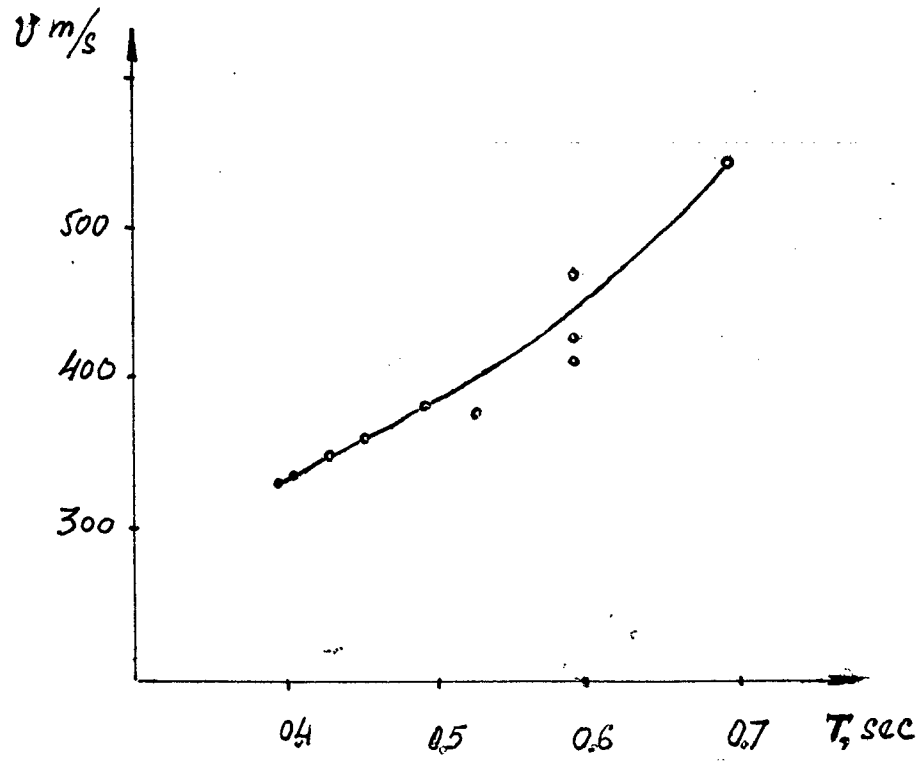

Figure 9. Phase velocity dispersion curve constructed from air-coupled surface wave period measurements and apparent acoustic wave velocity obtained from relative source/receiver positions.

ACOUSTIC OBSERVATIONS

Acoustic Wavetrain

In addition to the direct acoustic arrival described previously for the atmospheric explosions, there is another type of acoustic wave which was observed from the surface and tamped explosions. This is a quasi-harmonic acoustic wavetrain of long duration which is existed by surface wave components with phase velocity equal to the sound speed. The constant transfer of seismic energy into the acoustic wave from propagating surface waves with this phase velocity produces large amplitude acoustic wave signals with a dominant period equal to the period of the surface wave source. Moreover, since the amplitudes of the surface waves decrease with increasing distance, this transfer of energy is most effective near the source and, consequently, the main features of this acoustic wave are related to the surface wave characteristics of the medium in the near-source region.

Figure 10 presents the records of the acoustic wavetrains generated by the surface and tamped explosions at the distance of 21 km. The signal duration of 16 sec and period of 0.56 sec are approximately the same for all the records. The maximum amplitude of the oscillations depends on the yield and depth of burial. For example, the tamped explosion is almost as efficient as the surface blast of twice the yield, with amplitudes of 5.5 Pa and 6 Pa, respectively.

The observed period of oscillations of 0.56 sec is larger than one would expect from the averaged phase velocity dispersion curve of Figure 9. This suggests that the near-surface velocity structure in the source region of the records may be locally different from that beneath the stations. The deeper second layer appeares to be more laterally homogeneous, as indicated by the consistency of the Airy phase exitation. Thus, the acoustic wavetrain carries information about the velocity structure near the source.

The relative amplitudes of the direct airblasts and the

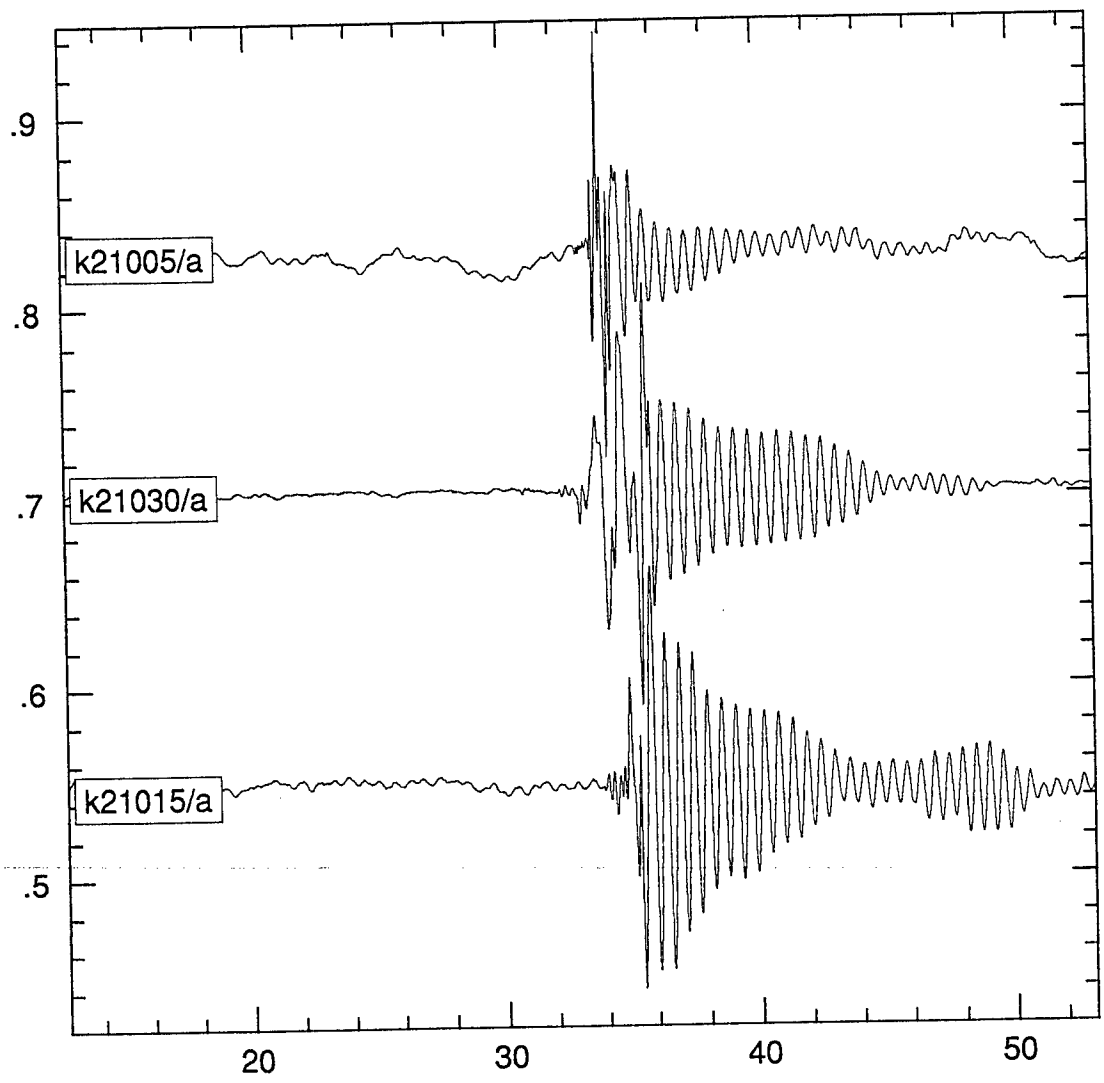

Figure 10. Acoustic wavetrains recorded at the distance of 21 km from the epicenters of surface and tamped blasts

following surface wave induced acoustic wavetrain can be used to discriminate between tamped and surface explosions.The amplitude of the direct airblast decreases rapidly with increasing depth, while the following acoustic wavetrain amplitude increases with depth of burial. Thus, for the contained explosion the direct airblast is almost absent (no ejection of gaseous products of detonation), while the coupled acoustic wavetrain is 2-3 times larger for the contained explosion than for the surface explosion which generates strong direct airblast signals.

Acoustic Precursor Nature

As was noted previously, the acoustic wave generated by the atmospheric and surface blasts in these experiment show evidence of a high frequency "acoustic precursor" which arrives before the main airblast signal associated with the expansion of gaseous detonation products. The predominant frequency of these precursory arrivals appears to be on the order of 100 Hz, although this value reflects the responce limitations of the acoustic sensors and is probably an underestimate. Our hypothesis is that this acoustic precursor is related to the supersonic ejection of shell splinters from the iron casing of the bomb. In this model, the precursory arrivals would corespond to a sequence of impulsive signals associated with the weak shock waves induced by the large number of shell fragments which are ejected from the detonation point with a wide range of directions and initial velocities.

The supersonic flight of a solid body in the air will generate a shock wave ahead of the tip with an amplitude which depends on the velocity and the shape of the body. The shock wave propagates in a Mach cone shape and has a velocity close to the sound speed due to the rapid decrease of amplitude with range. Deceleration due to air friction slows the body and when its velocity drops to the sound speed a shock wave is no longer exited. From this moment, a shock wave of cone shape expands independent of the nature of the body.

The shock wave generated in the ambient air by detonation

of explosives in the bomb decelerates more rapidly and lags behind the ejected debris. Simple consideration of the bomb blast as a point source in a homogeneous atmosphere (Kestenboim et al., 1974) shows that shock wave velocity for a 1000 kg explosion will be approximately $1.5c_a$ in 0.5 seconds and approximately $1.2c_a$ in 2 seconds after explosion.

The initial velocities of the shell splinters are estimated to be in the range 1.0-2.4 km/s. Supersonic flight with Mach velocity, M, of 3-7 will be decelerated by a frictional force proportional to M^2 (Landau and Livshitz, 1989). The velocity time history can be estimated from Newton's second law:

$$m\frac{dv}{dt}=\alpha v^2 \qquad (4)$$

where m is the body mass and α is a constant depending on the shape which can be can be estimated from the experimental data. Integrating Equation (4) from t=0 to time moment t we obtain velocity as a function of time in the form:

$$v(t)=\frac{mv_o}{v_o\alpha t+m} \qquad (5)$$

where $v(0)=v_o$, the initial velocity. The time/distance curve can be obtained by integrating Equation (5) to obtain:

$$S(t)=\frac{m}{\alpha}\ln\left(\frac{v_o\alpha}{m}t+1\right) \qquad (6)$$

Now the distribution of shell-splinter masses can be roughly evaluated from the total bomb weight and the number of impulse-like arrivals of shock wave associated with debris ejection. The total mass is about 500 kg with 100-150 fragments recorded. Thus, if the shell-splinter masses are distributed evenly in the range from 0.5 to 5 kg, we obtain a total mass of 500 kg. Field observations, in fact, showed that the

shell-splinters had this range of masses. The shapes of the observed bomb fragments were cubic to a first order of approximation. By using Equation (4), one can estimate α from the time delay of the main shock. For m=1 kg and a time of flight of 2 sec, the constant α is about 1.5. Thus, such a fragment decelerates to sonic velocity at a distance of 1.35 km from the detonation point and, at this time, the main shock front has only propagated to a range of 0.9 km, giving a predicted time delay of about 1.3 sec in good agreement with the observations. Moreover, the initial velocities of the larger fragments should be lower, which would explain the observed increase in precursor amplitude with time up to the arrival of the main shock.

There are several areas of potential applications of these acoustic precursor data. The first is related to an estimation of the total number of shell fragments. That is, by using a suitable sensor high-frequency sensor, it should be possible to resolve all the shocks and, hence, the number of fragments.

A second potential application is the detection of explosion-like acoustic sources in the atmosphere. Observations of such a precursor is a sign of supersonic debris ejection and unequivocally indicates an explosion source. Moreover, the relative time delay of such a precursor signal provides information regarding the initial velocity of the debris and may be used to evaluate explosive type.

METHODS OF ACOUSTIC SOURCE HEIGHT ESTIMATION FROM SEISMIC DATA

The processes of acoustic and seismic waves conversion at the free surface give rise to some relatively simple methods of acoustic source height estimation. These methods can be used for sources having significant hight (1-15 km) if they are detected by a regional seismic network in the distance range from 1 to 50 km. Of course, their application requires a local geological structure characterized by a near-surface sedimentary layer and a steep velocity gradient with depth, to ensure efficient generationof the Airy phase.

The first method is similar to that of proposed by Johnston (1987) and is based on epicentral location. If the seismological network detects air-coupled seismic waves, standard procedure of epicenter location can be employed. However, if Airy phase data are also detected, it is possible to estimate acoustic source height. The relative arrivals of air-coupled and Airy phases depend on the distance and height. The acoustic wave travel time is given by

$$t_a = \frac{(h^2+r^2)^{1/2}}{c_a} \qquad (7)$$

while the Airy phase travel time can be estimated from relationship

$$t_A = \frac{(h^2+r^2)^{1/2}}{c_a} + \frac{r-r}{V_A} \qquad (8)$$

where V_A is the group velocity of the Airy phase. Thus, using $t_a - t_A$ values from several stations, one can estimate r and h. Application of this technique to the present data gives a height estimate of 6.2 km for the explosion at 6 km height by interpolation of the results from the 4 and 8 km blasts.

The second method uses not only arrival times but also period information. We have established already that the

apparent acoustic wave velocity can be estimated from the phase velocity dispersion curve. Thus, the incident angle (the apparent velocity) can be estimated from the observed period of oscillations in the air-coupled surface wave, as well as the angle to the source. Using the arrival times of the air-coupled surface waves and the Airy phase as described above one can estimate epicentral distance. Then, the angle to the source and the epicentral distance determine the height.

The third method is based on single station data. Since the group velocity dispersion is evident in the air-coupled surface wave data, it is possible to estimate the apparent acoustic wave velocity and its spatial gradient near the receiver. These velocity and gradient data constrain height and epicentral distance through Equations (2) and (3).

The methods described above can be used in zones three and four where the Airy phase is separated from the air-coupled surface wave. Alternately, the signal duration and its spectral content in the second zone can be used for height estimation. Since the signal duration in this zone depends on source height and distance from reciever to the point where constructive interference starts in a complicated manner, we only note here the example of the different duration and spectral content for air blasts at different heights recorded at the range of 6 km (cf, Figure 6).

It is important that there are methods based on local characteristics of geological structure near the receiver. Thus, it is not necessary to consider complicated lateral variations of propagation path from the source to the receiver in order to obtain valid estimates. To some extent, the local structure can be treated as large scale sensor which amplifies the low amplitude signals of interest.

CONCLUSIONS

Scientists from the Institute for Dynamics of the Geospheres carried out a series of 8 explosive tests in December 1985 at a Soviet bombing range near Kustanai, Kazakhstan. The objective of the experiments was to record seismic and acoustic waves by blasts of different energy release at different heights. The charges were conventional bombs with total weights of 3000, 1500 and 500 kg. The chemical explosives constituted about 50% of the weights of the bombs. The series consisted of five 1500 height of burst tests (2 at 8 km, 2 at 6 km, 1 at 4 km) and three near-surface explosions with weights of 500, 1500 and 3000 kg. The 500 kg and 3000 kg explosions detonated on impact, while the 1500 kg explosion had a 1 sec delay which resulted in a penetration to a depth of about 15 m in the marshy soil. There were three observation points at ranges 6, 9.5 and 21 km. All three ground motion components (R, T, Z) were measured at all the three ranges. In addition, acoustic sensors (microphones) were installed at each point. At 6 km the sensor was at the top of a tower of about 7 m height. AT 9.5 km there were two sensors at heights of 1 and 13 m and at 21 km there were two different sensors at a height of about 1 m.

The seismic and acoustic data were measured by conventional oscilloscopes onto the photographic paper. At first, the data were digitized and converted into standard format to access the data processing options. All the digitized waveforms with proper description were assemled into a uniform database, which is available now to seismic verification community by prompt from the IDG. There are more than 50 3-C seismic and acoustic recordings.

The data processing included amplitude, period and spectral estimations of different seismic and acoustic phases, their interpretation and definition of the dependence of the observed characteristics on explosion yield, height of burst and the subsurface geology of the test area. The atmospheric and near-surface explosions generate different seismic phases. The most prominent are the air-coupled surface wave generated locally, and the Airy phase which propagates with alsmost

constant period and relatively low attenuation. The atmospheric explosions generate the air-coupled wave relatively more efficient than the near-surface with a ratio of the amplitudes of the waves being more than an order of magnitude higher from the atmospheric explosions. This feature shows evidence of difference between atmospheric and near-surface explosions.

Second prominent feature of the near-surface explosions is a large-amplitude acoustic wavetrain arriving after the first impulsive arrival. This wavetrain is generated near the sources by constructive interference induced by the surface wave harmonics with phase velocity equal to the sound velocity in the air. There is no such an arrival from the atmospheric explosions.

There is also another signature of the observed acoustic waves important for discrimination. The atmospheric explosions of the bombs generate a relatively intensive high-frequency precursor associated with supersonic ejection of shell splinters and related low amplitude impulses arrival. The contained explosion did not show such a signature due to no shell splinters ejected.

The observed seismic waves from the atmospheric explosions show a possibility of using them to estimate height of burst. There are some procedures of the HOB estimation proposed in the study based on arrival times of different phases, dispersion of the air-coupled wave, and time duration of the signals.

A phase velocity dispersion curve was estimated from the observed periods in the air-coupled wave and the apparent velocities of the acoustic wave along the free surface. The curve is consisted with a theoretical curve, calculated from the known velocity distribution in the local geological structure.

Spectral processing showed that the Airy phase has a period of about 1 sec consistent with the thickness of the sedimentary layer and seismic waves' velocities in the geological structure. The air-coupled wave is characterized by a variation of the periods due to changes of the apparent velocity of the acoustic front along the free surface.

REFERENCES

Berzon, I.S. and I.P.Pasechnik (1976). **Construction of Earth by dynamic characteristics of seismic waves. Investigation of crust and mantle.** Nauka, Moscow. (in Russian)

Ewing, W.M., W.S. Jardetzky and F.Press (1957). **Elastic waves in layered media.** McGraw-Hill, New-York.

Gubkin, K.E. (1976). On the similarity of explosions, Fizika Zemli (Earth's physics), No10, 49. (in Russian)

Johnston, A.C. (1987). Air blasts recognition and location using regional seismographic networks, Bull. Seismol. Soc. Am. 77, 146.

Kestenboim, H.S., G.S.Roslyakov and L.A. Chudov (1974). **Point explosion,** Nauka, Moscow. (in Russian)

Landau, L.D. and E.M. Livshitz (1989). **Hydrodynamics,** Theoretical physics vol.6, Nauka, Moscow, 640. (in Russian)

Murphy, J.R. (1981). Near-field Rayleigh waves from surface explosions, Bull. Seismol. Soc. Am. 71, 223.

Murphy, J.R. and H.K. Shah (1988). An analysis of the effects of site geology on the characteristics of near-field Rayleigh waves, Bull. Seismol. Soc. Am. 78, 64.

Press, F and J. Oliver (1955). Model study of air-coupled surface waves, J. Acoust. Soc. Am. 27, 43.

Werkle, H. and G. Waas (1987). Analysis of ground motion caused by propagating air pressure waves, Soil Dynamics and Earthquake Engineering 6, 194.

APPENDIX A.

There are more than 50 seismic and acoustic waveform measured during the experiment and then digitized from photographic paper and converted into SAC and CSS formats. These data are available by request from the Institute for Dynamics of the Geospheres, Moscow, Russia.

The data can be separated into two principal groups according to nature of the source: near-surface and atmospheric explosions. The surface explosions generated relatively more intensive Airy phase and the atmospheric explosions generated more intensive air-coupled surface wave.

The first group of the recordings is displayed in Figures A-1 through A-4. Unfortunately, only recordings at the 21 km station are available due to technical problems at the closer stations during these explosions. Figure A-1 shows acoustic and seismic waveforms from 0.5 ton explosion at the free surface. The acoustic waveform was measured near the free surface (at the height about 1m) and has a prominent quasi-sinusoidal wavetrain following by an impulse arrival generated by shock wave near the source. The wavetrain was exited near the source by the shock wave moving along the surface and should have phase velocity close to the apparent velocity of the shock wave along the surface. Since the shock wave decelerated when propagated, this wavetrain has a dispersive nature. Relative amplitudes of the impulse arrival and wavetrain are described in the report. The acoustic wave produces a sharp signature on the seismic records as clear from the seismic waveforms. The two seismic recordings are radial and vertical components. The acoustic effect is relatively more intensive on the vertical component. The Airy phase is the largest arrival on the both components, however. This phase is due to a sharp velocity gradient between the sedimentary and intrusive layers and propagates with alsmost constant period of about 1 sec. Since the Airy phase has group velocity higher than the acoustic wave it arrives before the acoustic wave. This might not be the case for the atmospheric explosions as will be shown later.

Figures A-2 through A-4 display similar features for the 1.5 and 3 ton explosions. There are some differences, however. These explosions generated the relatively less intensive acoustic wave with lower impulse arrival and almost no distinct signature of the impulse on the seismic records. This is due to penetration of the bombs into the ground. The impulsive arrival is of relatively higher amplitude from the 3 ton explosion, however, indicating shallower penetration and more efficient air-coupled wave generation. These features are used to characterize a possibility of the atmospheric, surface and underground explosions discrimination. P- and S-waves arrivals were measured only from the 3 ton explosion and were not analysed.

The second group of recordings is from the atmospheric explosions. Figures A-5 through A-18 display the acoustic and seismic waveforms according to increasing height of bursts and distance from the receivers. Some acoustic records are given in larger scale to show important features of the signals.

Figures A-5 through A-8 show the results of the measurements from the 1.5 ton bomb at all the three stations. At the 6 km station the most prominent phase is the air-coupled surface wave. This wave has a complex structure with a sharp inverse dispersion induced by deceleration of the apparent velocity of the acoustic wave along the free surface. No harmonic of the surface wave has high enouth group velocity to go ahead of the acoustic wave at this distance. At the 10 km station (Figure A-6) this wave pattern is changed. Low-frequency surface wave goes ahead of the air-coupled seismic wave. The acoustic front arrives about 2 seconds later and generates the air-coupled wave. The acoustic recordings are given in detail in Figure A-7. High-frequency oscillations can be seen on the recordings associated with shell splinters ejection. The waveform k10415/ah was measured at the height of 13 m and has two distinguished peaks associated with incident and reflected waves. The incident and reflected wave amplitudes are close and near the groud (k10415/a) generate a wave with twice as large amplitude. At the 21 km station, wave pattern is more clear with

the air-coupled surface wave and Airy phase separated. The acoustic wave has an impulse character and has no distinct high-frequency precursor due to lower frequency band of the measuring sensor. The air-coupled surface wave is generated more efficiently at the vertical component.

Figures A-9 through A-11 show the recordings from the 6 km explosion. The wave-fields are similar to those of from the 4 km explosion. The only significant difference is a smaller lag of the air-coupled wave relative to the Airy phase at the 10 km station.

Figures A-12 through A-18 display the recerdings for the two explosions at 8 km. The results of the measurements from the two explosions are very close showing a stability of all the conditions. In general, the results are close to those observed from the 4 and 6 km explosions. There are some fine differences, of course, which are analized in the report and used to estimate their HOB.

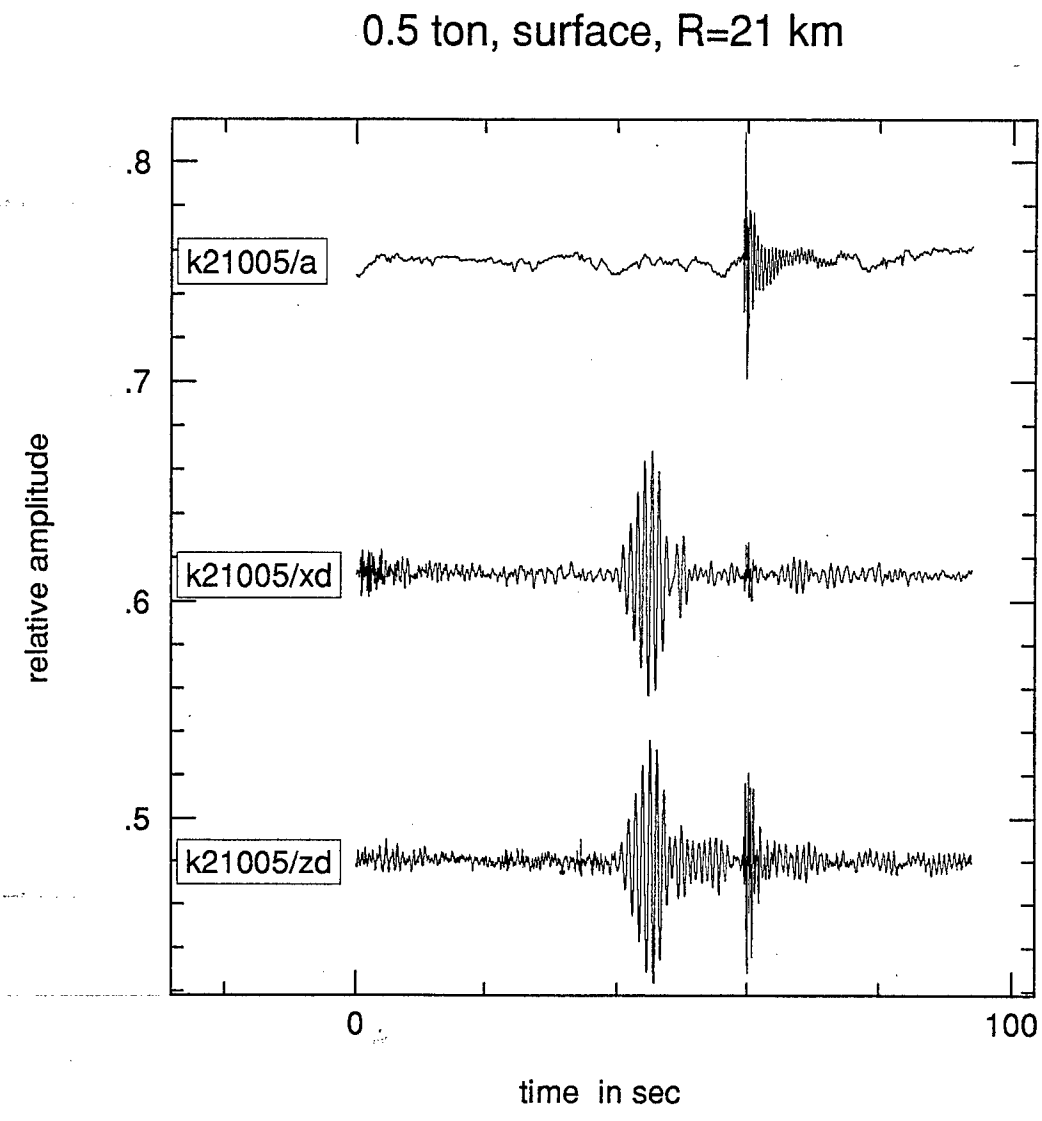

Figure A-1. Acoustic (k21005/a) and seismic (k21005/xd - radial, and k21005/zd) waveforms recorded from the 0.5 ton explosion at the surface at the 21 km station. The acoustic wavetrain is generated by surface wave near the source. The Airy phase is of the highest amplitude on the both vertical and radial seismic waveforms. The acoustic front effect can be seen on the seismic records. (Scales of the waveforms are independent).

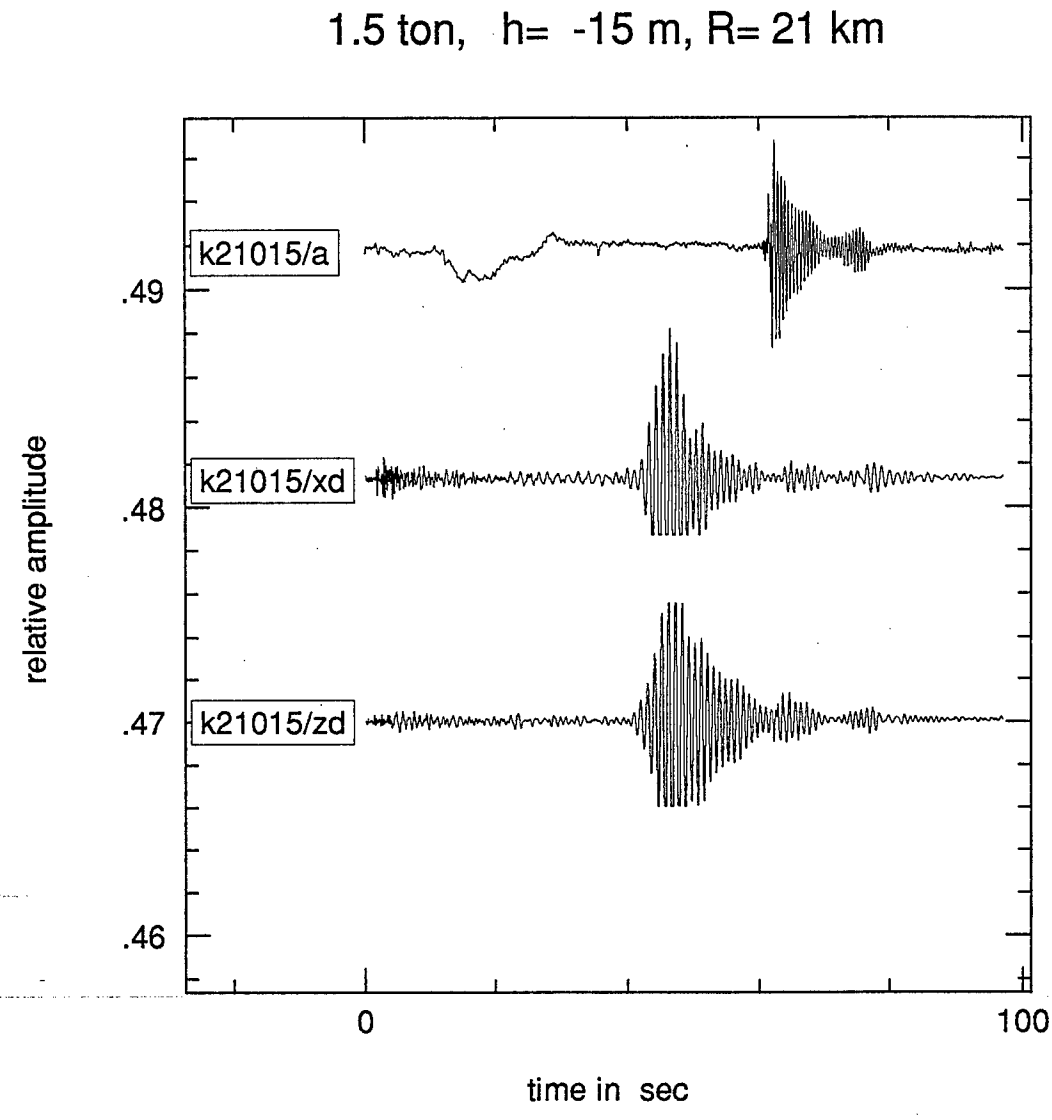

Figure A-2. Acoustic (k21015/a) and seismic (k21015/xd - radial, and k21015/zd) waveforms recorded from the 1.5 ton explosion at depth of 15 m at the 21 km station. The acoustic wavetrain is generated by surface wave near the source. The Airy phase is of the highest amplitude (clipped) on the both vertical and radial seismic waveforms. The acoustic front effect is not seen on the seismic records. (Scales of the waveforms are independent).

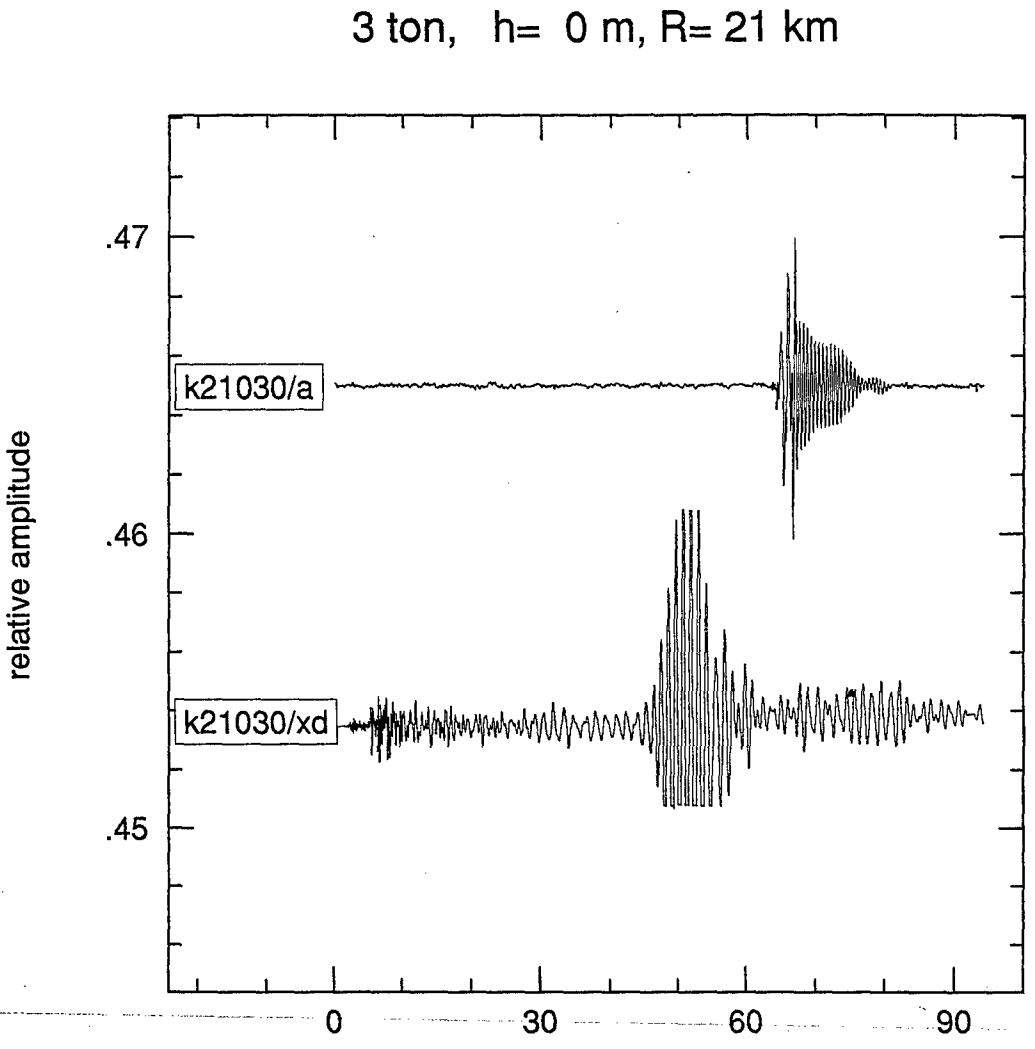

Figure A-3. Acoustic (k21030/a) and seismic (k21005/xd - radial) waveforms recorded from the 3.0 ton explosion at the surface at the 21 km station. The acoustic wavetrain is generated by surface wave near the source. The impulse acoustic arrival is of higher amplitude than the wavetrain . The Airy phase is of the highest amplitude on the both vertical and radial seismic waveforms. The acoustic front effect can be seen on the seismic record. (Scales of the waveforms are independent).

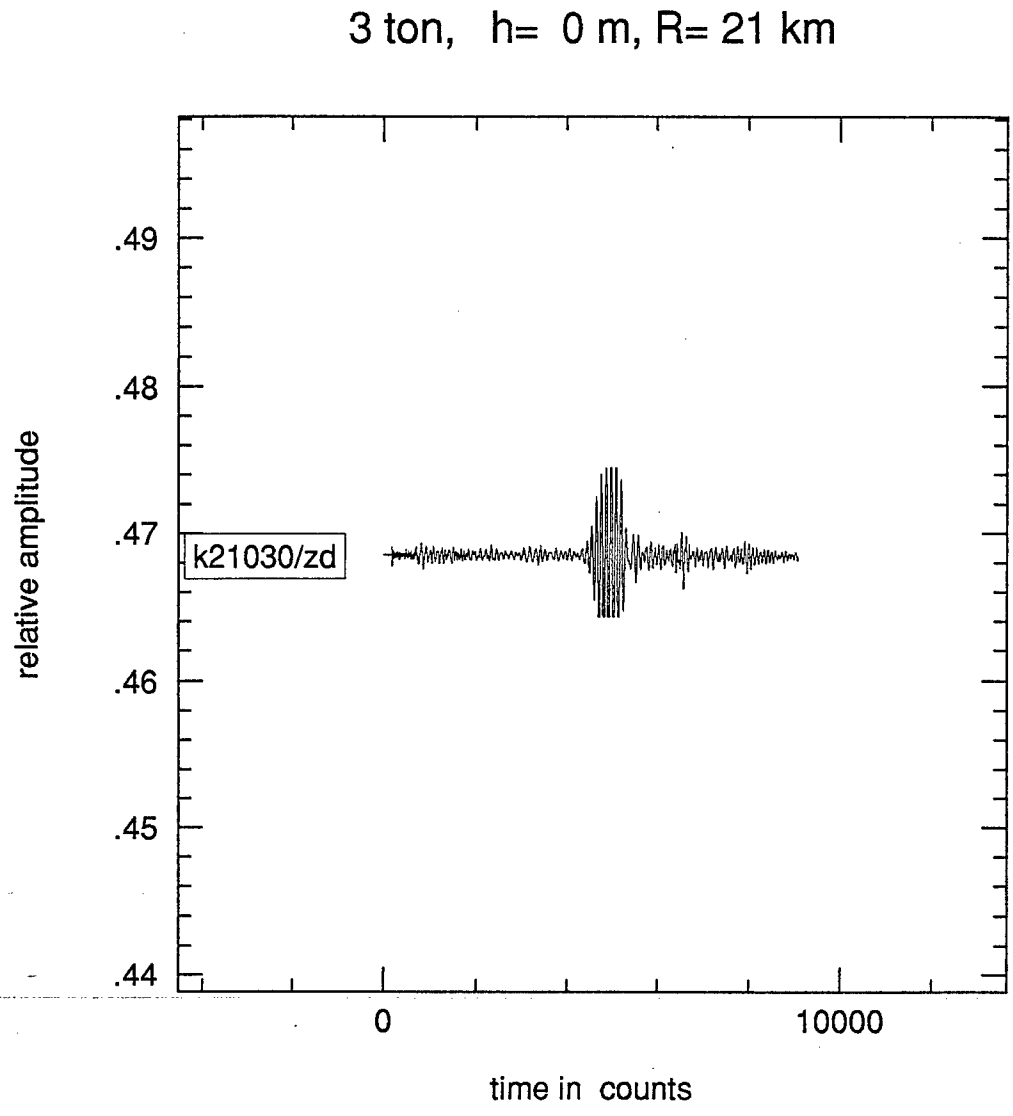

Figure A-4. Seismic (vertical - k21005/zd) waveform recorded from the 3.0 ton explosion at the surface at the 21 km station.

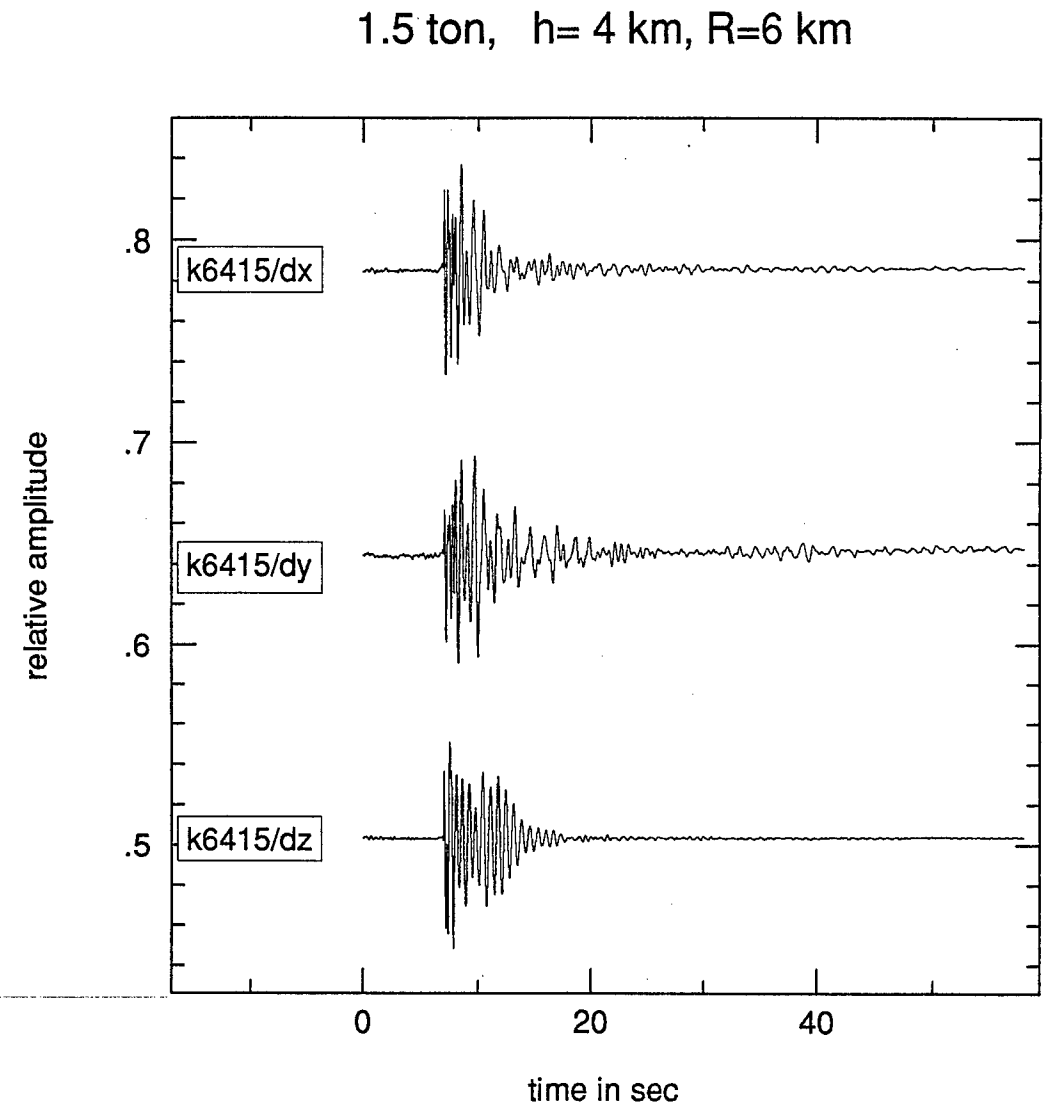

Figure A-5. Seismic waveforms (three component) recorded at the 6 km station from the 1.5 ton explosion at the height 6 km. The air-coupled seismic phase is of the highest amplitude.

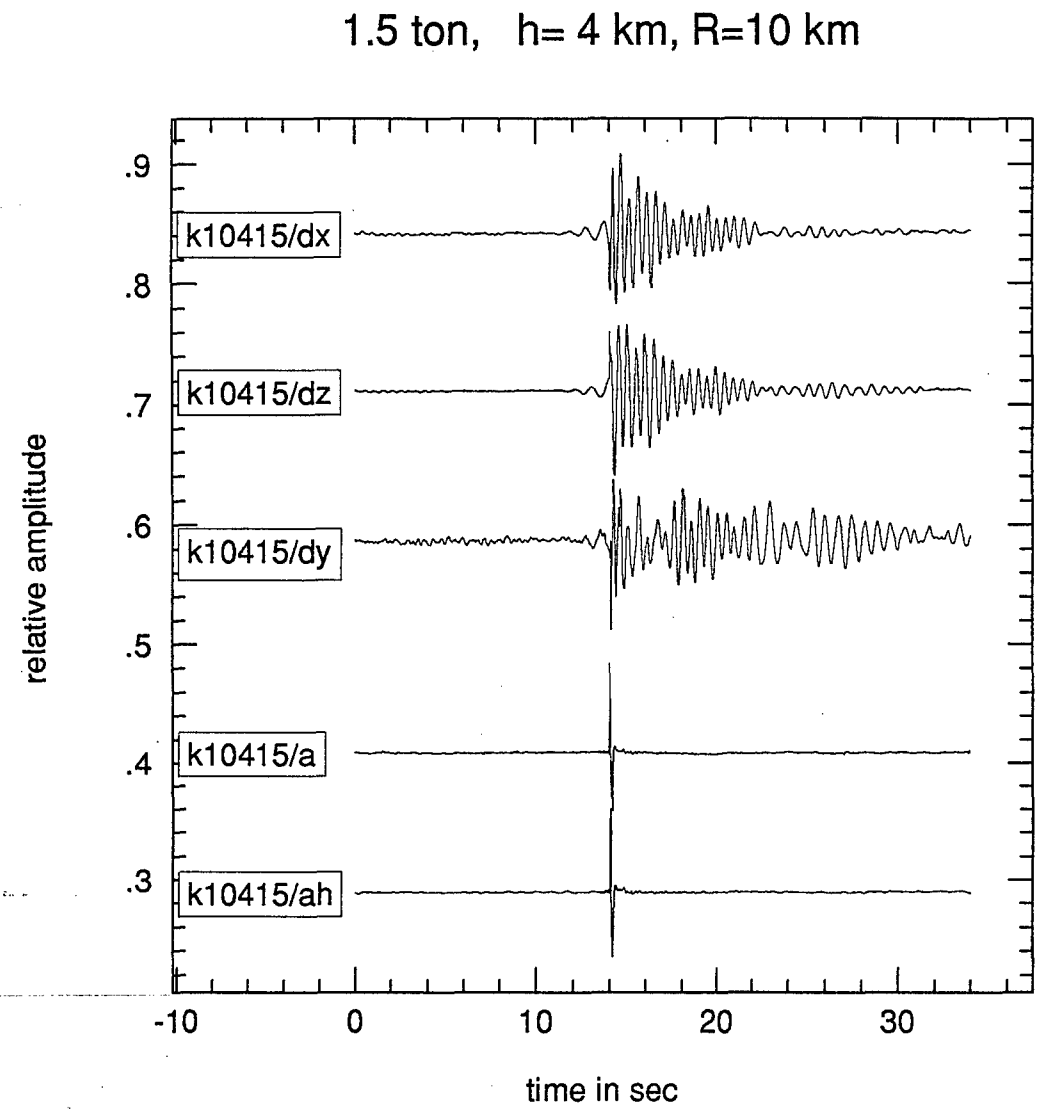

Figure A-6. Seismic (three component) and acoustic waveforms (k10415/a - at height 1 m, k10415/ah - at height 13 m) recorded at the 10 km station from the 1.5 ton explosion at the height 4 km. The air-coupled seismic phase is of the highest amplitude. Surface wave goes ahead of the air-coupled wave.

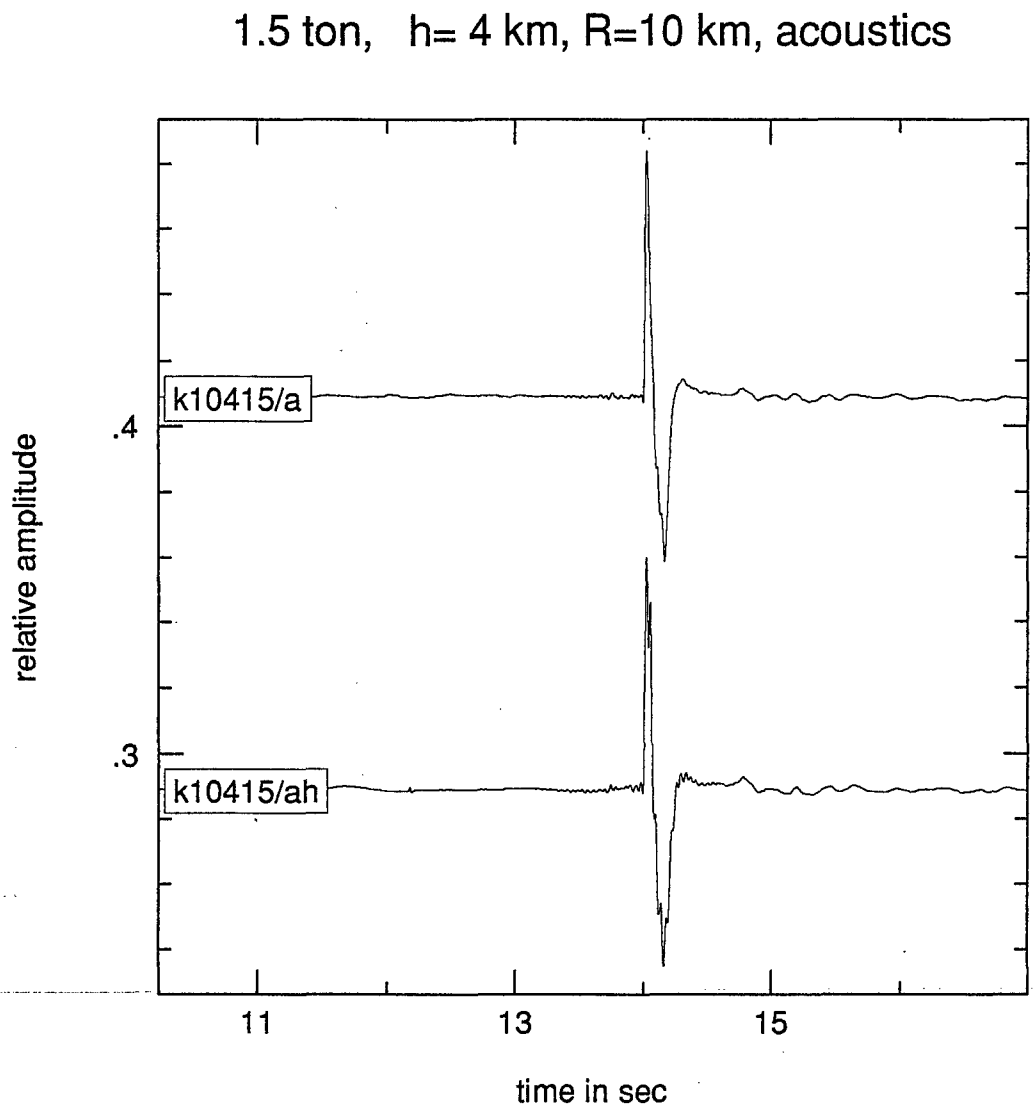

Figure A-7. The two acoustic waveforms from Figure A-6 enlarged (scales independent). High-frequency precursor can be seen on the records.

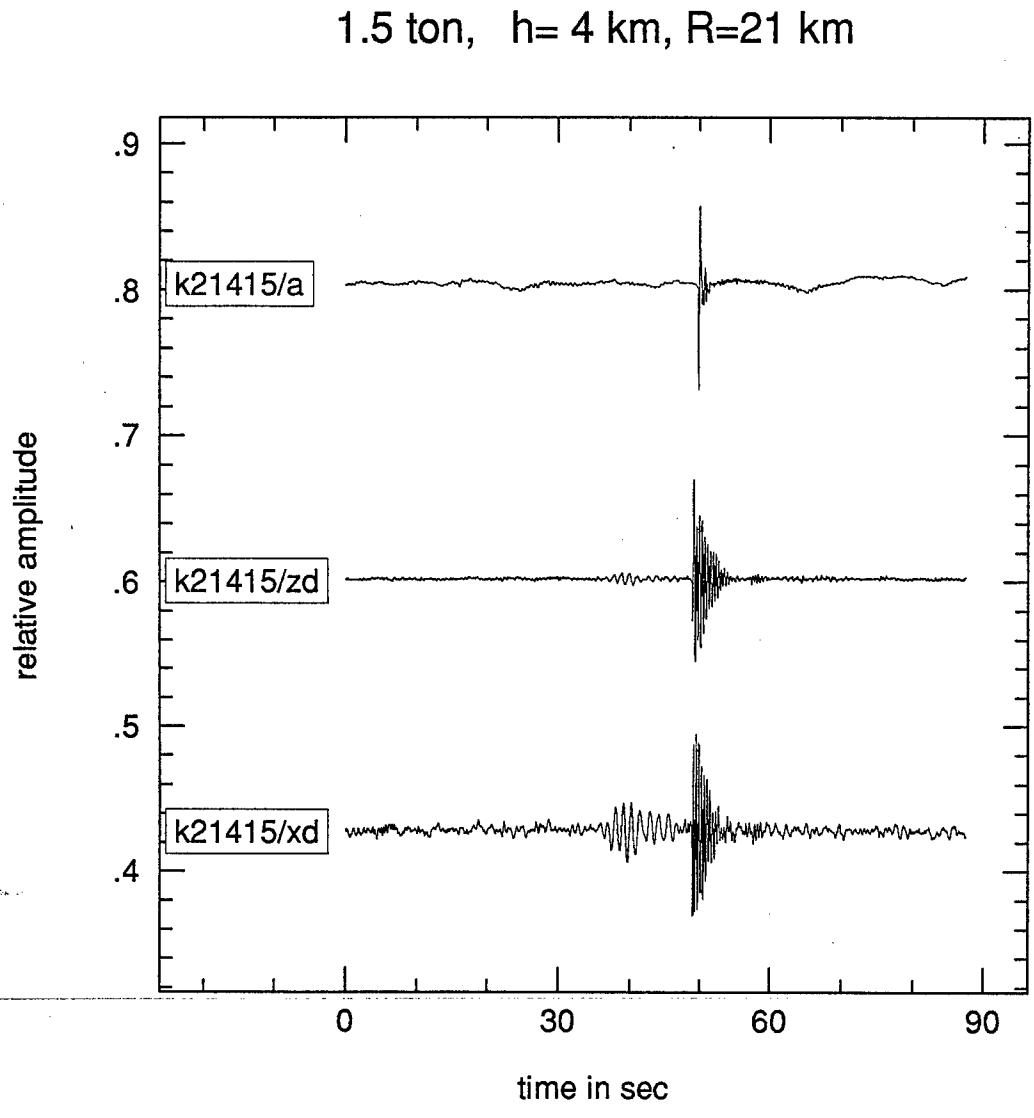

Figure A-8. Acoustic and seismic (vertical and radial components) waveforms recorded at the 21 km station from the 1.5 ton explosion at the height 4 km. The air-coupled seismic phase is of the highest amplitude.The Airy phase and air-coupled wave are separated with the latter being of larger amplitude.

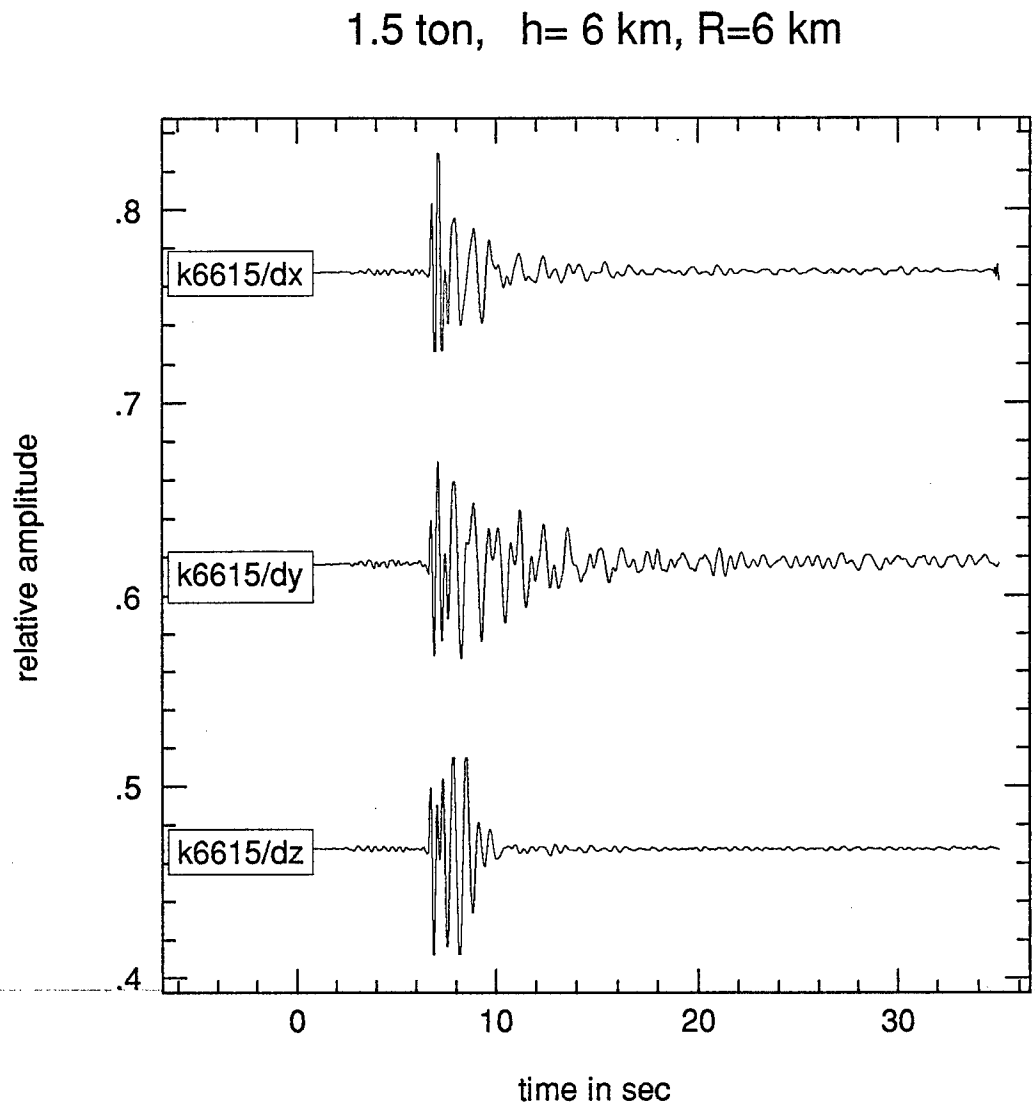

Figure A-9. Seismic waveforms (three component) recorded at the 6 km station from the 1.5 ton explosion at the height 6 km. The air-coupled seismic phase is of the highest amplitude.

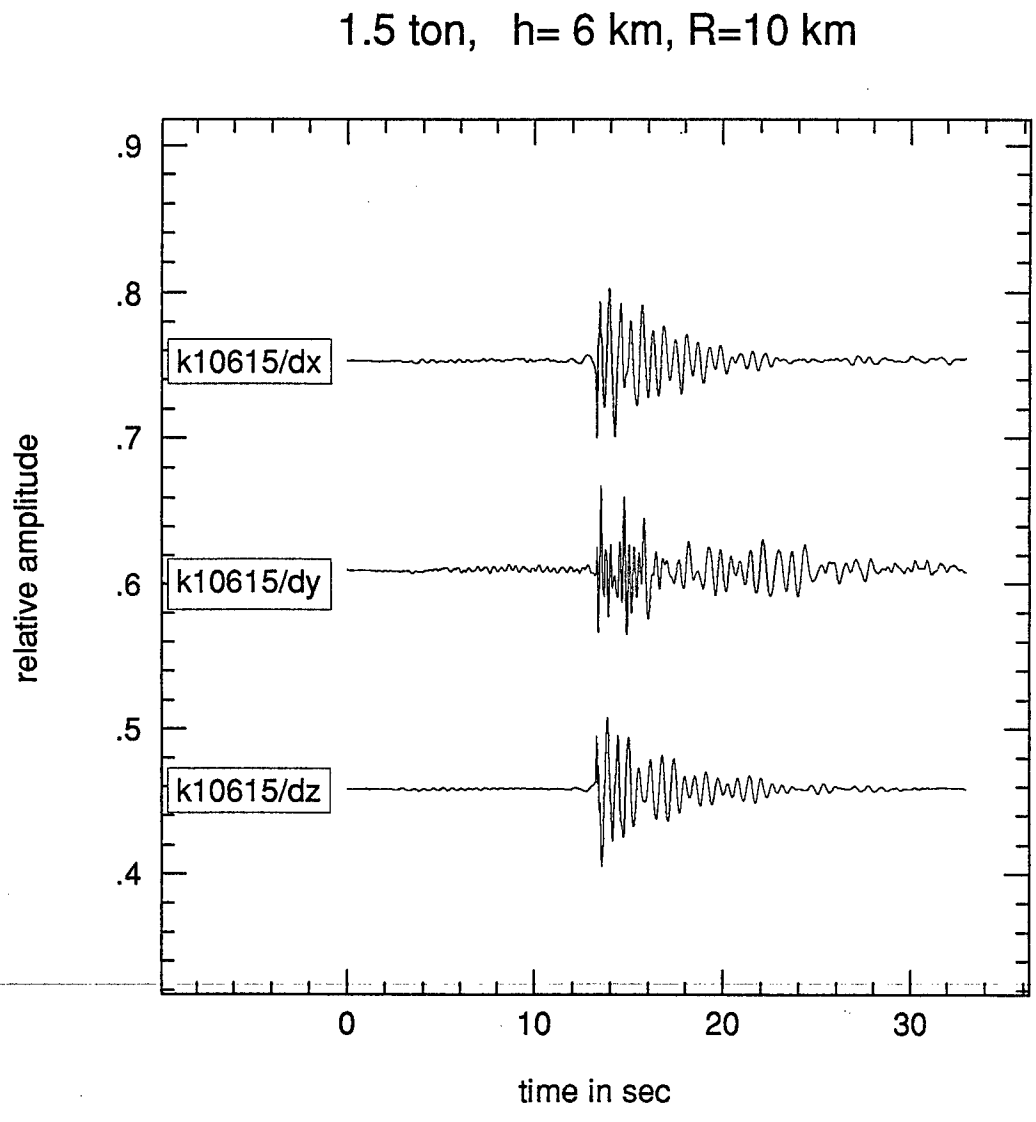

Figure A-10. Seismic waveforms (three component) recorded at the 10 km station from the 1.5 ton explosion at the height 6 km. The air-coupled seismic phase is of the highest amplitude. Surface wave starts to go ahead of the air-coupled wave.

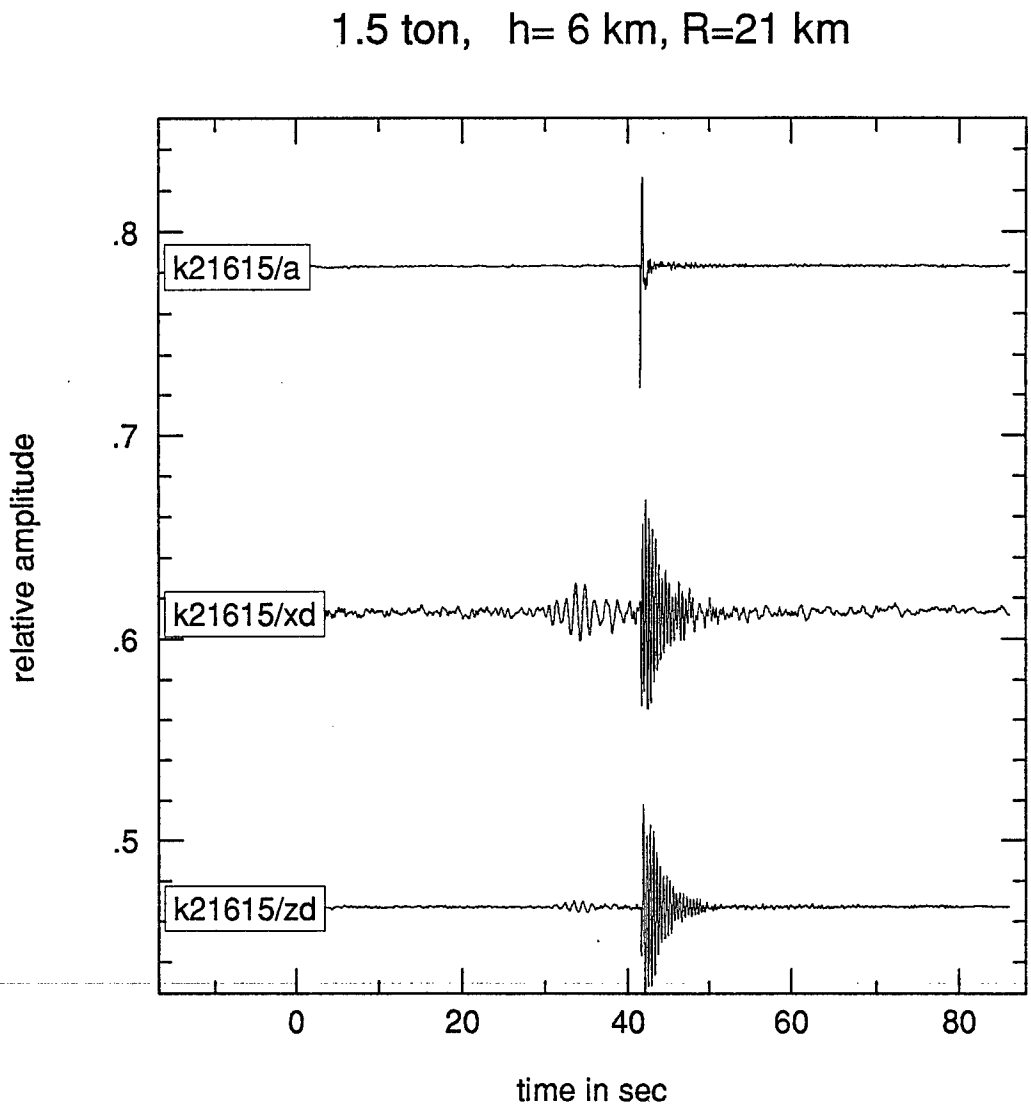

Figure A-11. Acoustic and seismic (radial and vertical components) waveforms recorded at the 21 km station from the 1.5 ton explosion at the height 6 km. The air-coupled seismic phase is of the highest amplitude. The Airy phase and air-coupled waves are separated in time.

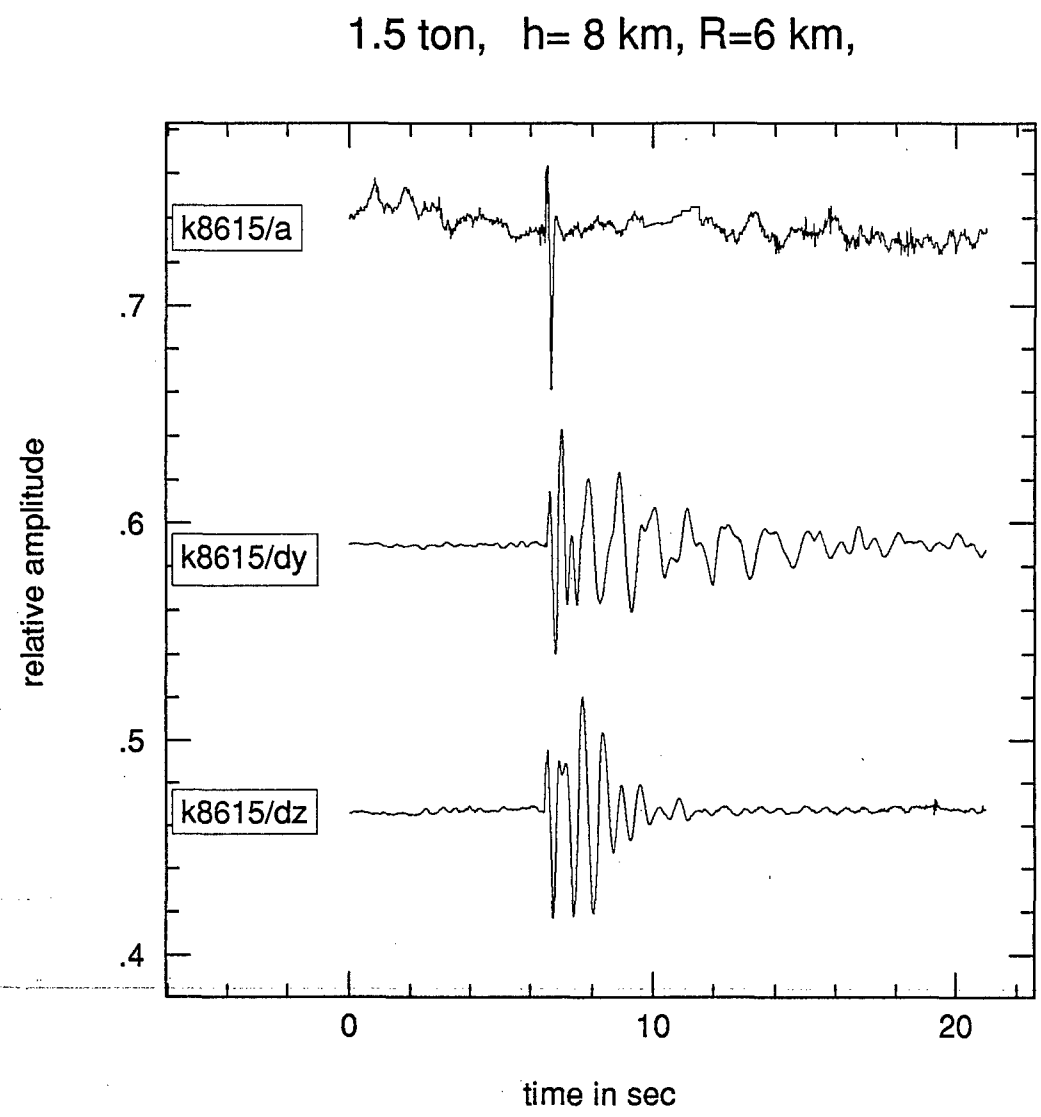

Figure A-12. Acoustic and seismic (transverse and vertical components) waveforms recorded at the 6 km station from the 1.5 ton explosion at the height 8 km. The air-coupled seismic phase is of the highest amplitude.

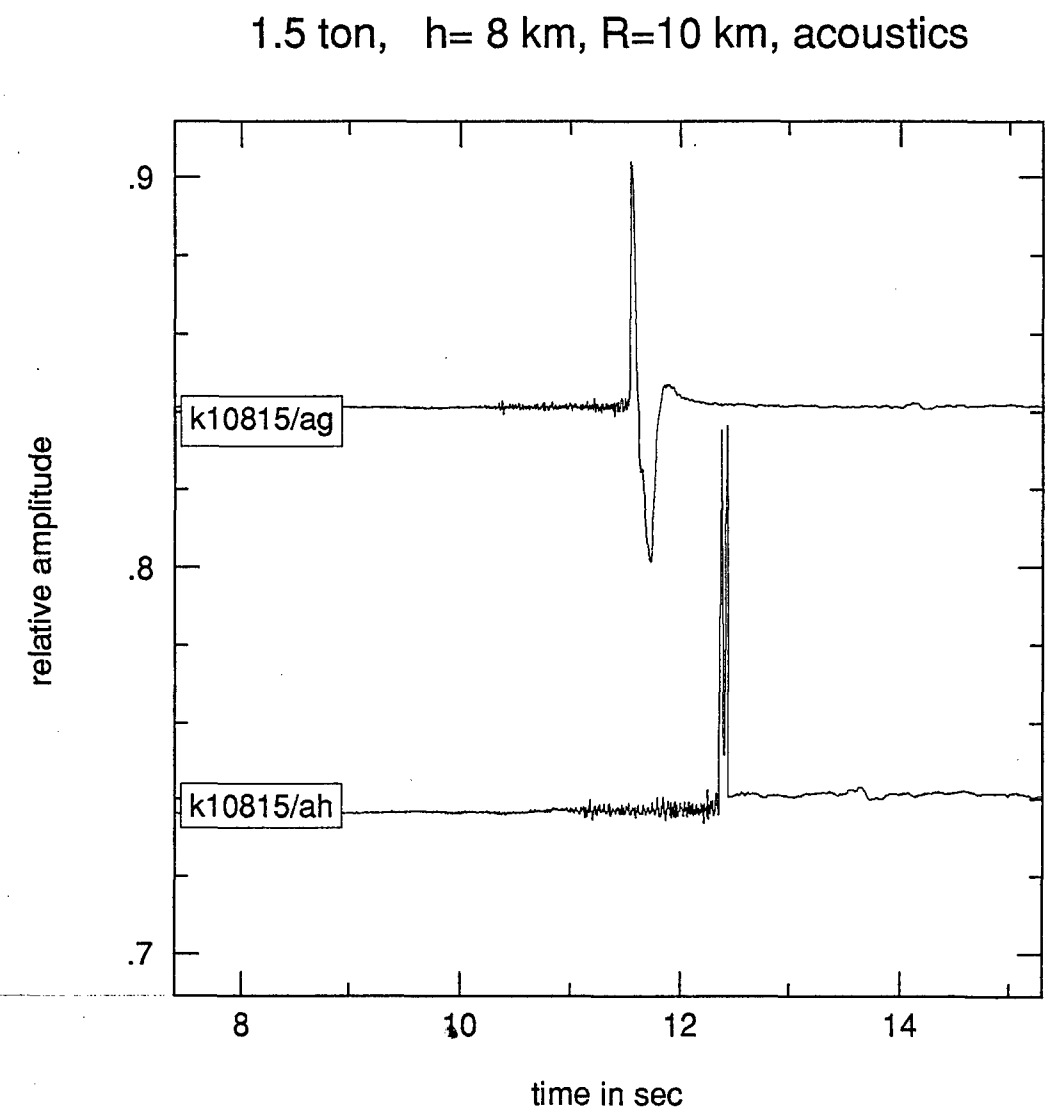

Figure A-14. Acoustic waveforms fron Figure A-13 enlarged. The high-frequency precursor is seen. Incident and reflected waves create double-peak structure.

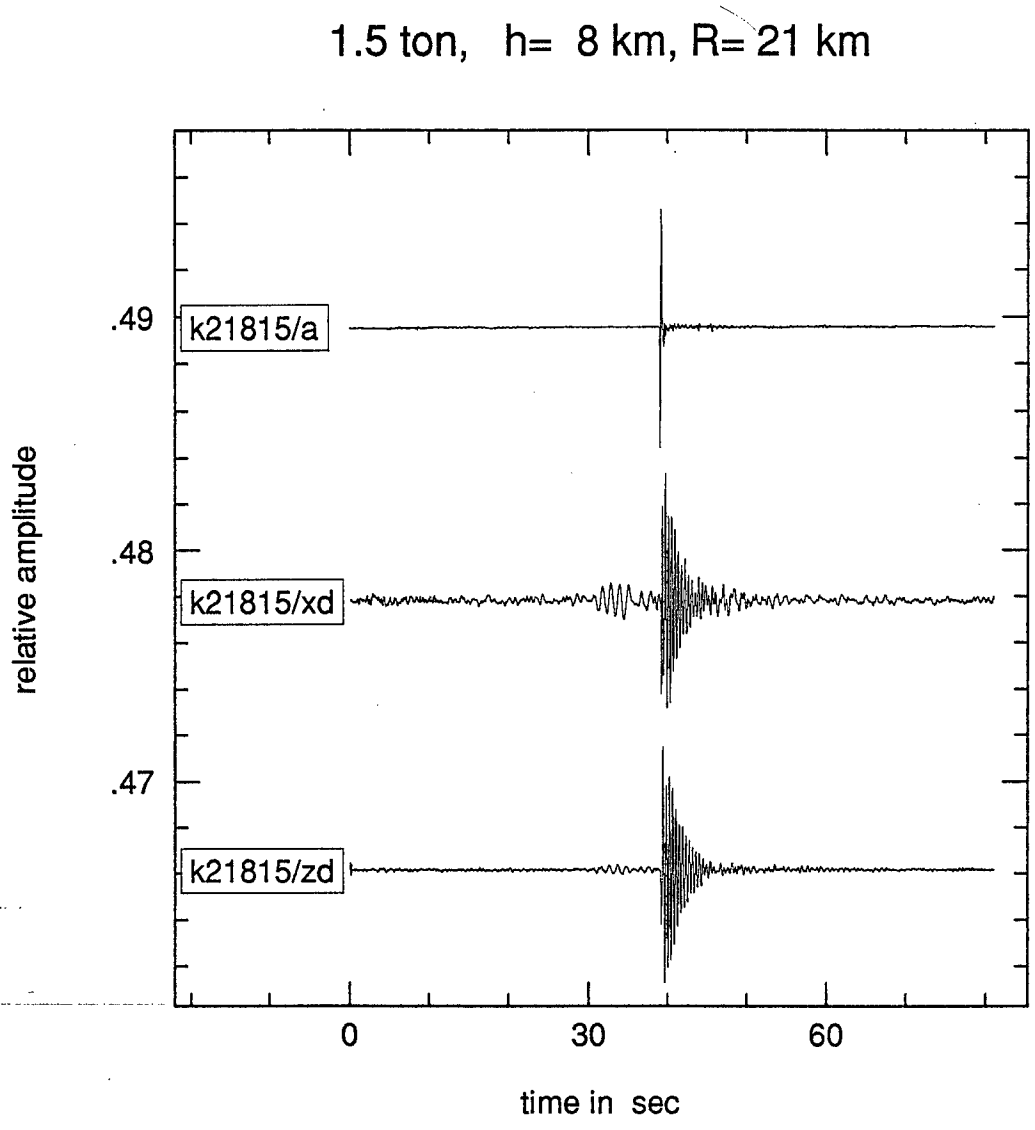

Figure A-15. Acoustic and seismic (radial and vertical components) waveforms recorded at the 21 km station from the 1.5 ton explosion at the height 8 km. The air-coupled seismic phase is of the highest amplitude. The Airy phase and air-coupled waves are separated in time.

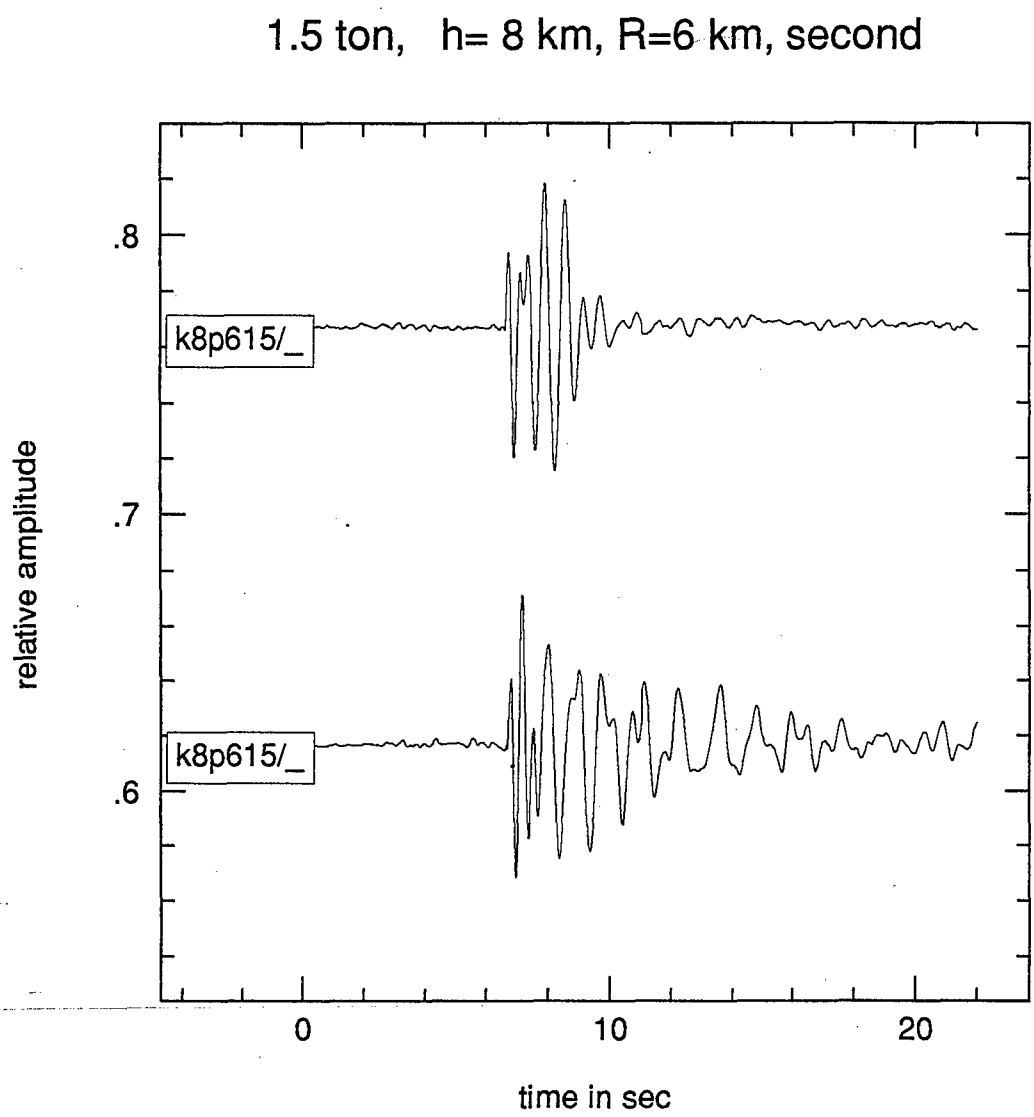

Figure A-16. Seismic (radial - lower, and vertical - upper components) waveforms recorded at the 6 km station from the second 1.5 ton explosion at the height 8 km. The air-coupled seismic phase is of the highest amplitude.

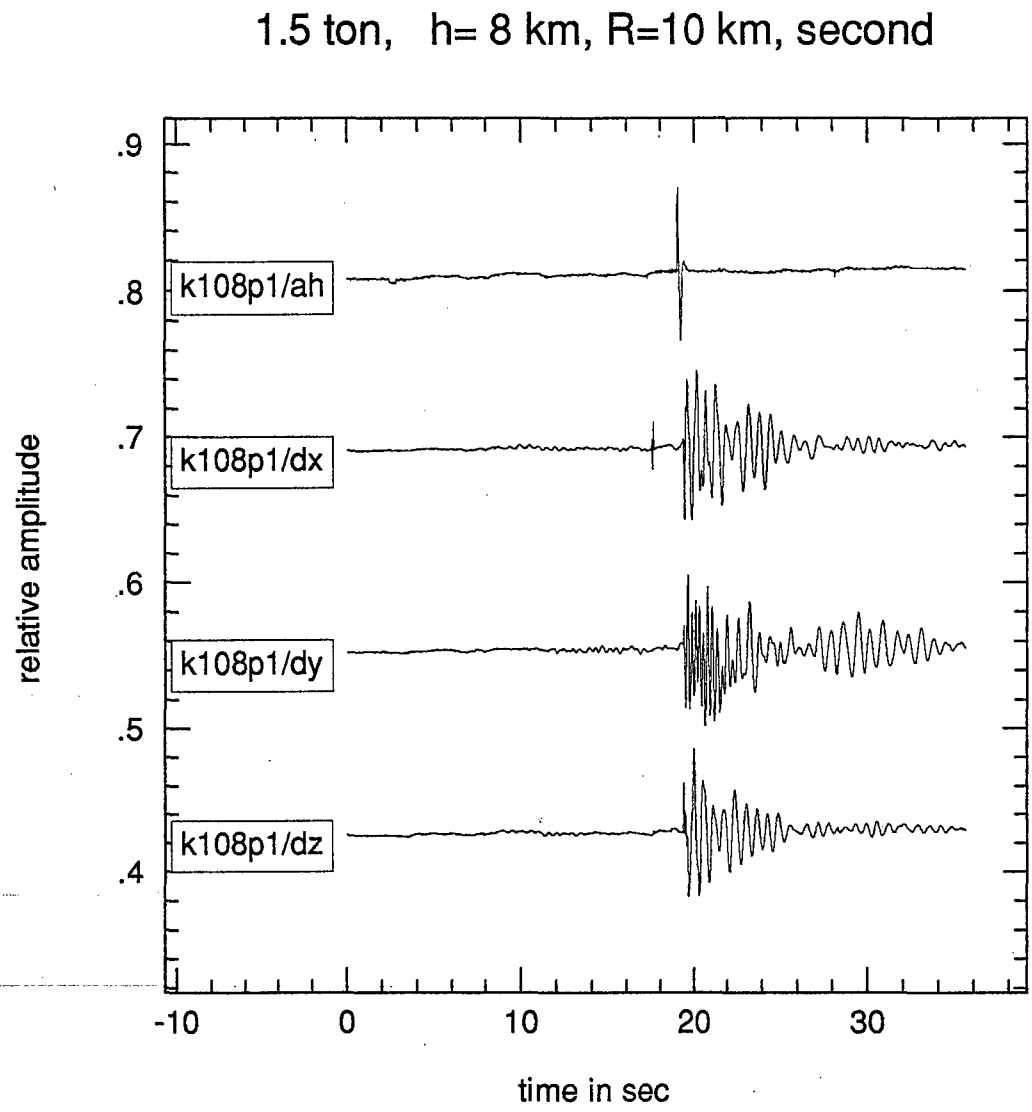

Figure A-17. Acoustic and seismic (three components) waveforms recorded at the 10 km station from the second 1.5 ton explosion at the height 8 km. The air-coupled seismic phase is of the highest amplitude.

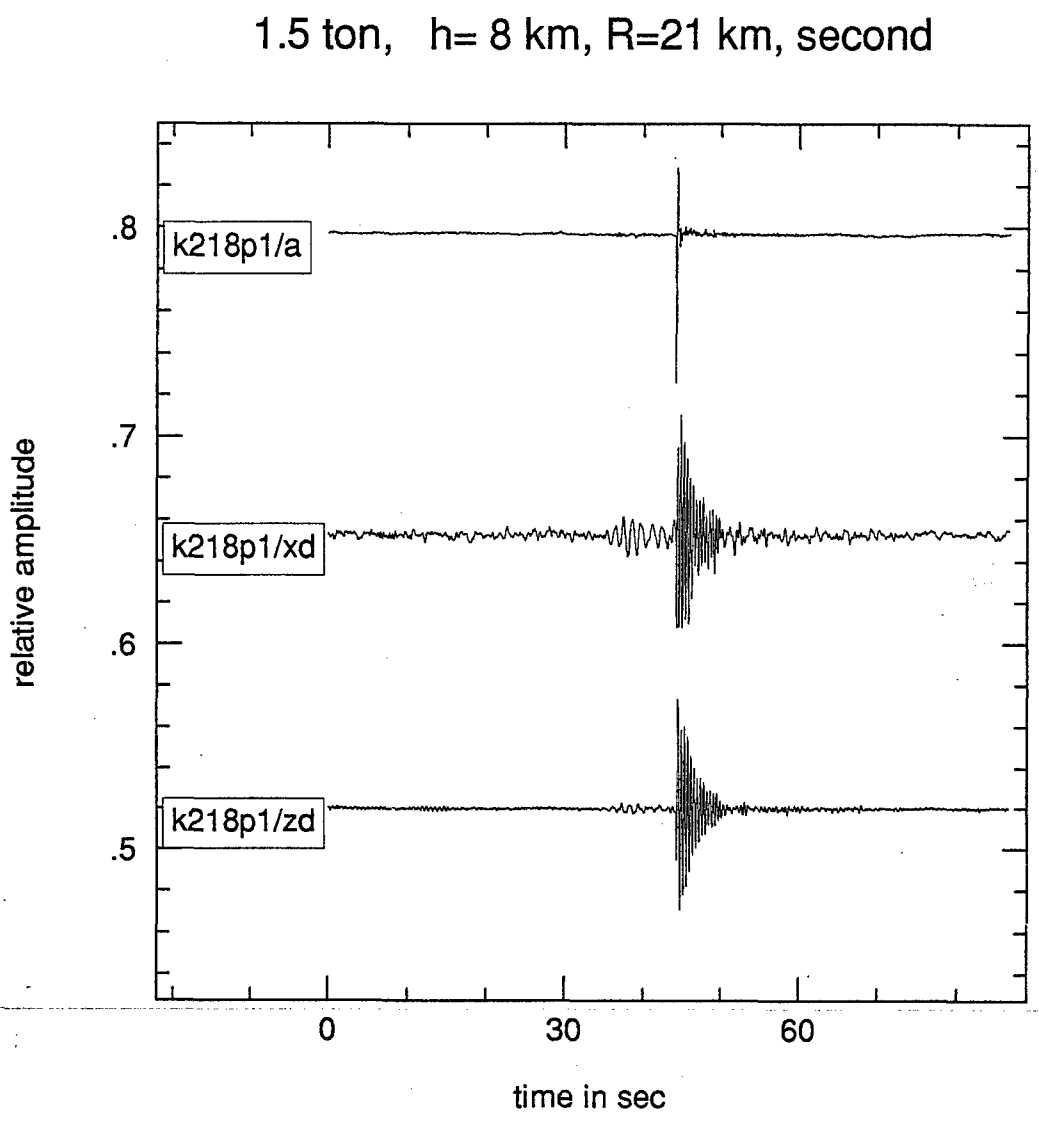

Figure A-18. Acoustic and seismic (radial and vertical components) waveforms recorded at the 21 km station from the second 1.5 ton explosion at the height 8 km. The air-coupled seismic phase is of the highest amplitude and separated from the Airy phase.